MICHIGAN STATE
UNIVERSITY

National Superconducting Cyclotron Laboratory

QUASIELASTIC KNOCK-OUT OF CLUSTERS BY ELECTRONS AND NUCLEAR RESTRUCTURING EFFECTS

ALEXANDER SAKHARUK, VLADIMIR ZELEVINSKY, and V.G. NEUDATCHIN

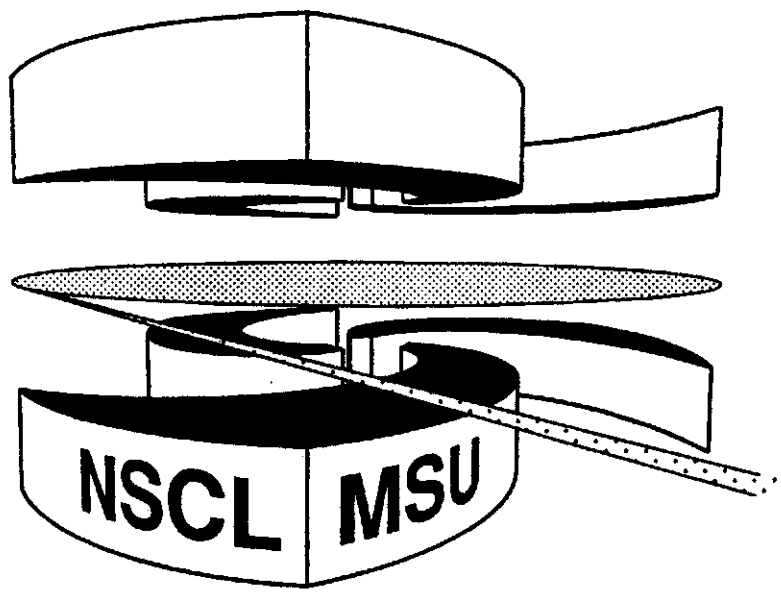

MSUCL-1124 MARCH 1999

QUASIELASTIC KNOCK-OUT OF CLUSTERS BY ELECTRONS AND NUCLEAR RESTRUCTURING EFFECTS

Alexander Sakharuk

National Superconducting Cyclotron Laboratory, Michigan State University,

East Lansing, MI 48824-1321 USA

and Brest State University, Brest 224665 Belarus

Vladimir Zelevinsky

National Superconducting Cyclotron Laboratory, Michigan State **University,**

East Lansing, MI 48824-1321 USA

V.G. Neudatchin

Institute of Nuclear Physics,

Moscow State University, Moscow 119899 *Russia*

(March 4, 1999)

The general microscopic formalism is presented for the description of the quasielastic knock-out of α - clusters from p - shell nuclei by ultrarelativistic electrons. Manifestations of nuclear structure in differential cross sections and angular distributions are studied. The typical $^{12}C(e,e'\alpha)^{8}Be$ reaction is considered in the PWIA and DWIA approximations; the particular attention is paid to the effects of virtually excited cluster states inside the initial nucleus. Suggestions for the observation of nuclear restructuring effects (interplay between diagonal and off-diagonal transitions with respect to the intrinsic state of the cluster) are proposed.

I. INTRODUCTION

Cluster structure of atomic nuclei is usually studied in two types of complementary experiments. Cluster transfer reactions [1] are characterized, as a rule, by high energy resolution and give reliable relative values of spectroscopic factors. The absolute values are not equally accurate due to complexities [2] inherent to the distorted wave Born approximation (DWBA) used for theoretical interpretation of experimental data. It is difficult to extract the most interesting object of such studies, the wave function of relative motion of the transferred cluster in the initial nucleus, in the region of relatively low momenta.

The second, and the most direct, type of experiments is the quasielastic (quasifree) knock-out reactions [2–7]. These reactions are distinguished by a number of tangible experimental shortages: one needs high beam energy, the counting rate in coincidence experiments is typically low, and the energy resolution is not sufficient. But the wave function of cluster relative motion in the target nucleus is extracted in the broad range of momenta. In addition, as we show below, the signatures of virtually excited nucleon cluster configurations [8–10] are most noticeable in the quasielastic knock-out reactions.

The quasielastic knock-out reactions at sufficiently high energies are particularly attractive because of the domination of the simplest pole reaction mechanism [11] and, henceforth, the possibility of the accurate extraction of quantitative spectroscopic information. Currently, an overwhelming majority of experiments are set up with the use of low or intermediate energy (200-300 MeV) proton beams. The theoretical analysis of experimental data is carried out in the framework of the simplest plane wave impulse approximation (PWIA) or with the more realistic distorted wave impulse approximation (DWIA) [12]. Both approaches utilize the factorization of the reaction cross section [2–7] which imposes serious limitations on the allowed states of the cluster inside the target nucleus. To be exact, it is assumed that the cluster was already preformed inside the nucleus in the same state as it had after the reaction being registered in coincidence with the projectile. This assumption can be reasonable at relatively low beam energy when the reaction is localized at the surface

region of the target nucleus. However, at high energies the cluster may be knocked out from a deep interior inside the target [4,13]. In this case the cluster can be formed in an arbitrary quantum state allowed by the conservation laws and selection rules. Therefore, the reaction cross section cannot be expressed in a simple factorized form [10,14]. The problem of calculating the cross section for the quasielastic knock-out (p,p'α) reaction, with cluster deexcitation amplitudes (nondiagonal amplitudes describing the intrinsic reorganization of the cluster) properly accounted for, was addressed in our previous works [14–17] in the framework of Glauber multiple scattering theory [18]. The final state interaction between the knocked out cluster and the residual nucleus was taken into account in the standard DWIA approximation [20]. The calculations have revealed a number of nontrivial peculiarities of the reaction. It turned out that the momentum distribution of the residual nuclei strongly depends upon the angle of the scattered proton and the orientation angle of the recoil momentum of the residual nucleus with respect to the initial beam and the proton scattering plane.

The use of electron beams for similar quasielastic knock-out experiments [14–17] has well known advantages [21–23]: (i) the reaction mechanism may be well separated from nuclear structure effects; (ii) light and medium nuclei can be studied without a noticeable distortion by the electromagnetic field (the final state interaction is essential only between the knocked out cluster and the residual nucleus and can be taken into account with the aid of the usual optical model); (iii) at a given energy transfer one can independently vary the momentum transfer. From the viewpoint of extracting the cluster properties, the main attractive feature is the possibility of seeing the signatures of the deexcitation amplitudes connected with the spin-isospin rebuilding of the cluster internal wave function. The restructuring of the spin-isospin part of the cluster wave function is suppressed in the (p,p'α) reactions due to a weak dependence of the nucleon-nucleon scattering amplitude on spin variables [10,18] at high proton beam energy which is necessary for the manifestation of the quasielastic reaction mechanism. In the electron induced reactions this mechanism reveals itself most clearly at energy E_e exceeding 400 MeV [23] although even at much lower energy ($\sim$100 MeV) one

can study specific features of (e,e'α) processes [19].

At the same time the use of reactions induced by electrons implies a number of difficulties as compared to the hadron analogs: (i) the reaction cross sections are substantially lower and therefore the requirements to experimental accuracy are considerably increased; (ii) since the electron scattering is a single-step interaction with one of the cluster nucleons, the elastic amplitude falls down rapidly as the momentum transfer increases. The first problem can be solved by progress in the electron beam and target technology. In particular, the method of superthin internal nuclear targets in an electron storage ring [19] is promissing, especially for the coincidence experiments. The second feature of electron experiments is important for our specific goals because, compared with the multiple proton scattering, the contribution of the deexcitation ampliudes to the total reaction cross section is significantly smaller. Moreover, anisotropy of the angular distributions of emitted α-particles with respect to the direction of the momentum transfer, found for the (p,p'α) reaction [15,16], is absent here (see Sec. 4 and Figs. 8-10). This puts a heavier load on theoretical calculations of the cross sections.

The present work is apparently the first attempt to estimate the influence of internal restructuring of the knocked out cluster on the observable (e,e'α) cross sections. The choice of the α - cluster is natural because this is a sufficiently large multiparticle system possessing a wide spectrum of virtual excitations. The lighter clusters, such as deuterons or ^{3}He, have only few deexcitation amplitudes, and their influence on the reaction cross section is expected to be weaker [10]. Nevertheless, we need to note that the simplest deexcitation process ^{12}C(e,e')^{10}B*(0^+,T=1) with the spin-isospin rebuilding of the virtual singlet deuteron e+d*(S=0,T=1)$\rightarrow$e'+d(S=1,T=0) has been investigated experimentally [24]. The theoretical description of this reaction within a semi-microscopic approach allowing the restructuring of the knocked out deuteron cluster was developed in [25]. The results indicate an importance of taking into account the deexcitation amplitudes. More traditional approaches like DWIA cannot reasonably describe available experimental data.

Recently a series of experiments was carried out at NIKHEF to study the knock-out (e,e'α) reactions on ^{12}C and ^{16}O nuclei [26]. Below we have chosen as an object of investiga-

tion a particular reaction ^{12}C(e,e'α)^{8}Be which is an electron analog of the proton knock-out reaction ^{12}C(p,p'α)^{8}Be studied earlier [15–17]. Here we have an opportunity to compare different reaction mechanisms and distinguish more clearly effects due to the cluster structure of the target nucleus. In addition, the residual nucleus ^{8}Be has relatively low rotational levels $2^+(E_x$=2.9 MeV) and $4^+(E_x$=11.4 MeV) that can be populated in the interaction process.

In order to closely approach the conditions of the NIKHEF experiment, we calculate the reaction cross section as a function of the scattered electron energy (the energy sharing experiment). We give the angular distributions too because they are sensitive both to the deexcitation amplitudes and to the variations of kinematical conditions.

In Sec. 2 of the paper, the basic microscopic formalism is developed which takes into account the nondiagonal transition amplitudes with the intrinsic restructuring of the knocked out α - cluster. Since the main attention is given to the observable effects of the nondiagonality, the reaction mechanism is treated here in the simplest PWIA approximation. Sec. 3 is devoted to the analysis of the modification caused by the distortion in the exit channel. The final state interaction is taken into account in the framework of the traditional DWIA approach. In Sec. 4 the results of the numerical calculations of differential cross sections and angular distributions are presented and discussed for different final states of the residual nucleus. The perspectives for further studies are discussed in Conclusion.

II. THE (E,E'α) REACTION IN THE PWIA

Throughout the work we use the following notations: A is the target nucleus; A_0 is the cluster knocked out from the target; A_1 is the residual nucleus; e is the unit positive charge. The usual metric with the signature $(+\ -\ -\ -)$ is assumed [27], and the natural unit system with c=1 and $\hbar$=1 is used. All calculations are carried out in the laboratory system.

A. Kinematics

The kinematic scheme of the reaction is shown in Fig. 1(a), and the corresponding Feynman diagram is depicted in Fig. 1(b). The notations for involved four-momenta are: initial electron $k^\mu \equiv (E_e, \mathbf{k})$; final electron $k'^\mu \equiv (E'_e, \mathbf{k}')$; momentum transfer $q^\mu = k^\mu - k'^\mu \equiv (\omega, \mathbf{q})$; target nucleus $P_A^\mu \equiv (M_A, 0)$; cluster inside the target nucleus $p^\mu \equiv (E_0, \mathbf{p})$; knocked out cluster in the final state $p'^\mu \equiv (E'_0, \mathbf{p}')$, and the residual nucleus $P_{A_1}^\mu \equiv (E_1, \mathbf{P_1})$. Quantities p, k ,k', ... are the absolute values of the three - dimensional vectors $\mathbf{p}$, $\mathbf{k}$, $\mathbf{k}'$, ... The scalar four - momenta product is $k^\nu \cdot k'_\nu \equiv (k \cdot k')$.

For definitiveness, we choose the kinematic conditions for the quasielastic knock-out of the α - particle from the target nucleus ^{12}C as in the NIKHEF experiment [26]. The energy of the initial electron beam is E_e=637 MeV so that all calculations can be carried out in the ultrarelativistic approximation for the electron. The electron scattering angle θ'_e is fixed at 26.06°; α - particles are registered at 71.08° with respect to the beam direction, see Fig. 1(a).

The kinetic energy of knocked out α - particles T_α falls almost linearly from $\approx$100 MeV to zero, Fig. 2(a), in the most interesting for our purpose energy range 500$\leq E'_e \leq$626 MeV for all transitions into different states of the residual nucleus. In the vicinity of the quasielastic peak for the transition into the ground state 0^+ of the residual nucleus ^{8}Be, T_α is close to 30 MeV. The momentum transfer varies insignificantly in this region, the typical value being around 283 MeV/c. The exact position of the quasielastic peak on the energy scale E'_e for three possible transitions is seen in Fig. 3 where the momentum of the residual nucleus ^{8}Be is shown. By definition, the quasielastic peak is fixed by the condition $\mathbf{P_1}$=0. Displaying a typical signature of the quasielastic mechanism, the angle $\theta_{^8Be-q}$ between the momentum of the residual nucleus $\mathbf{P_1}$ and the momentum transfer $\mathbf{q}$, Fig. 2(c), changes abruptly from 180° to zero at the crossover through the quasielastic peak on the energy scale. Figs. 2(b) and 2(d) show additional kinematic reaction characteristics, E_{rel}, the energy of relative motion of the knocked out α - particle and the residual nucleus ^{8}Be, and the angle between $\mathbf{p_{rel}} = \mathbf{p}' - \mathbf{P_1}$ and $\mathbf{q}$, respectively. These quantities are important for calculating the cross section with

distortion in the exit channel because they determine the choice of parameters of the optical α - ^{8}Be potential.

B. Differential cross section

The electromagnetic interaction between the electron (projectile) and the target nucleus is given [22,23,27] by the operator

$$\hat{V}(t) = -e \int J^{\mu}(x) A_{\mu}(x) d\,\mathbf{r}, \tag{1}$$

where $x \equiv (t, \mathbf{r})$ and $J^{\mu}(x)$ is the four-vector of the nucleon current. The four-potential of the electromagnetic field of the electron $A^{\mu}(x)$ can be found from the Maxwell equation in the Lorentz gauge. In the lowest order of perturbation theory (one-photon exchange) we obtain the well-known Möller potential [22,23,28] for the electron transition $(\mathbf{k}, \sigma) \to (\mathbf{k}', \sigma')$

$$A^{\mu}(x) = -\frac{4\pi}{(q \cdot q)} \overline{u}_{\sigma'}(\mathbf{k}') \gamma^{\mu} \mathbf{u}_{\sigma}(\mathbf{k}) \mathbf{e}^{-\mathbf{i}(\mathbf{q}\cdot\mathbf{x})}. \tag{2}$$

Here $u_{\sigma}(\mathbf{k})$ are the electron Dirac bispinors normalized according to $\overline{u}_{\sigma}(\mathbf{k})\mathbf{u}_{\sigma'}(\mathbf{k}) = (\mathbf{m/E})\,\delta_{\sigma\sigma'}$; m is the electron mass. This normalization is not relativistically covariant but it is suitable in nonrelativistic nuclear physics.

Taking into account the connection between $\hat{V}(t)$ and the $\hat{S}$ - matrix [27] one obtains the process amplitude as

$$S_{fi} = -\frac{4\pi i e}{(q \cdot q)} \overline{u}_{\sigma'}(\mathbf{k}') \gamma_{\mu} \mathbf{u}_{\sigma}(\mathbf{k}) \cdot \mathbf{2}\pi\delta(\mathbf{E_0'} + \mathbf{E_1} - \mathbf{M_A} - \omega) \mathbf{J}^{\mu}_{\mathfrak{fi}}(\mathbf{q}), \tag{3}$$

where the transition four-current is

$$J^{\mu}_{fi}(\mathbf{q}) \equiv (\rho_{\mathfrak{fi}}(\mathbf{q}), \mathbf{J}_{\mathfrak{fi}}(\mathbf{q})) = \langle \mathbf{f} | \int \mathbf{e}^{\mathbf{iq\cdot r}} \mathbf{J}^{\mu}(\mathbf{r}) \mathbf{dr} | \mathbf{i} \rangle, \tag{4}$$

and the functions $|i\rangle$ and $|f\rangle$ describe the internal states of the nuclear system before and after interaction, correspondingly. The integration in the matrix element is done over all nucleon coordinates $\boldsymbol{r}_j$ (j=1,...,A) in an arbitrary coordinate system. Extracting center-of-mass motion by means of the transformation to standard Jacobi coordinates [13] and introducing the scattering amplitude T_{fi} [27],

$$T_{fi} = -\frac{4\pi ie}{(q \cdot q)} \overline{u}_{\sigma'}(\mathbf{k}')\gamma_\mu \mathbf{u}_\sigma(\mathbf{k}) \cdot (\mathbf{2\pi})^4 \mathbf{J}^\mu_{\mathfrak{fi}}(\mathbf{q}), \tag{5}$$

we obtain

$$S_{fi} = i(2\pi)^4 \delta^{(3)}(\mathbf{p}' + \mathbf{P_1} - \mathbf{q}) \delta(\mathbf{E'_0} + \mathbf{E_1} - \mathbf{M_A} - \omega) \mathbf{T}_{\mathfrak{fi}}, \tag{6}$$

In Eq. (5) and below, the internal states of the nuclear system $|i\rangle$ and $|f\rangle$ depend upon the Jacobi coordinates only. We use the same notations as in (3) for the new states in order to avoid an excessive overload of formulas. All information about center-of-mass motion is now contained in the δ - function which reflects the momentum conservation law.

The differential cross section of the $A(e, e'A_0)A_1$ reaction is related to the scattering amplitude [22,23,27,28] and, for the unpolarized electron beam and target nucleus, may be written as

$$\frac{d\sigma}{d\Omega'_0 d\Omega'_e dE'_e} = \frac{1}{2J+1} \sum_{M_J, M_{J_0}, M_{J_1}} \frac{1}{2} \sum_{\sigma,\sigma'} \frac{E_e p'^2 k' E'_e}{k} f |T_{fi}|^2. \tag{7}$$

Here J is the target spin (full angular momentum), and M_J its projection; M_{J_0} and M_{J_1} are projections of the spins (full angular momenta) of the knocked out cluster and residual nucleus, respectively. The factor f takes into account the recoil of the residual nucleus [3],

$$f = \left| \frac{p'}{E'_0} + \frac{p' - q\cos\gamma}{E_1} \right|^{-1}, \tag{8}$$

where γ is the angle between $\boldsymbol{p}'$ and $\boldsymbol{q}$, see Fig. 1(a).

After averaging over electron polarizations [27] we obtain the well known [23,29] differential cross section (7) of the quasielastic knock-out of the cluster A_0 from the target nucleus A,

$$\begin{aligned} \frac{d\sigma}{d\Omega'_0 d\Omega'_e dE'_e} = & \frac{1}{2J_A+1} \sum_{M_{J_A}, M_{J_0}, M_{J_1}} \frac{e^2}{4\pi^3} \frac{1}{(q\cdot q)^2} \frac{p'^2 k'}{k} f \\ & \times \{\rho_{fi}\rho^*_{fi} k'k(1+\cos\vartheta_e) + \mathbf{J}_{\mathfrak{fi}} \cdot \mathbf{J}^*_{\mathfrak{fi}} \mathbf{k}'\mathbf{k}(1-\cos\vartheta_e) \\ & + 2\mathrm{Re}\left[(\mathbf{J}_{\mathfrak{fi}} \cdot \mathbf{k})(\mathbf{J}^*_{\mathfrak{fi}} \cdot \mathbf{k}')\right] - 2\mathrm{Re}\left[\mathbf{J}^*_{\mathfrak{fi}} \rho_{\mathfrak{fi}} (\mathbf{k}\mathbf{k}' + \mathbf{k}'\mathbf{k})\right]\}. \end{aligned} \tag{9}$$

The whole information on nuclear structure is contained in the transition charge density $\rho_{fi}(\mathbf{q})$ and the transition current density $\mathbf{J}_{\mathfrak{fi}}(\mathbf{q})$.

In the energy region $E_e \sim 600$ - 650 MeV and for the analyzed transitions $^{12}C(J^\pi = 0^+; T = 0) \rightarrow ^8Be(J^\pi = 0^+, 2^+, 4^+; T = 0)$, the dominating contribution to the reaction cross section comes from the Coulomb part of the electromagnetic interaction $\rho_{fi}(\boldsymbol{q})$. The contribution of the current components $\boldsymbol{J}_{fi}(\boldsymbol{q})$ does not exceed $3\% \div 5\%$ and becomes visible mainly through its interference with the Coulomb part. We have performed direct calculations of this contribution for the transition into the ground state of the residual nucleus ^{8}Be at three different E'_e values around the quasielastic peak. As usual, the convective and magnetic components of the current were taken into account [23]. We do not expect any significant enhancement of the current components for the transitions into ^{8}Be excited states which have collective rotational nature. Therefore, below we restrict ourselves with the detailed consideration of the Coulomb interaction between the electron and those nucleons of the target nucleus that form the α - cluster.

We use in our calculations the charge density operator [23]

$$\hat{\rho}(\mathbf{q}) = \mathbf{e}\sum_{\mathbf{j=1}}^{\mathbf{A_0}} \mathbf{e}^{\mathbf{iq\cdot r_j}} \frac{\mathbf{1}}{\mathbf{2}}[\mathbf{1} + \tau_{\mathbf{3}}(\mathbf{j})]\mathbf{F}(\mathbf{q}_\mu^2)\delta(\mathbf{r} - \mathbf{r_j}), \tag{10}$$

where $F(q_\mu^2)$ is the electromagnetic form-factor of a free proton parametrized in the same way as in [30]. For brevity we omit the form-factor $F(q_\mu^2)$ in the explicit expressions but it was included in all numerical calculations.

C. Wave function of the target nucleus

The wave function $|i\rangle$ of the target nucleus ^{12}C with total spin J and isospin T is taken in the intermediate coupling scheme [13],

$$|i\rangle = \sum_{[f],L,S} a^{A,JT}_{[f]LS} |(1s)^4(1p)^{A-4}[f]^{(2T+1)(2S+1)} L_J\rangle. \tag{11}$$

Each component in (11) can be decomposed, with the help of the fractional parentage coefficient (fpc) techniques [13], into components containing intrinsic wave functions of the α - cluster and the residual nucleus, and a function of their relative motion. Particular

values of coefficients $a^{A,JT}_{[f]LS}$ obtained by the diagonalization of the nucleon-nucleon interaction Hamiltonian were taken from [31]. The basis functions in Eq. (11) are

$$|(1s)^4(1p)^{A-4}[f]^{(2T+1)(2S+1)}L_J\rangle \equiv |AN[f]LSJTM_JM_T\rangle =$$

$$= \sum_{\substack{N_1,[f_1],L_1,S_1,J_1,T_1,\Lambda,\mathcal{L},\\ N_0,[f_0],L_0,S_0,J_0,T_0,j,n}} \langle AN[f]LST|A_1N_1[f_1]L_1S_1T_1;n\Lambda,A_0N_0[f_0]L_0S_0T_0\{\mathcal{L}\}\rangle$$

$$\times (-1)^{\Lambda+L_0+j+S_0}\sqrt{(2J_1+1)(2j+1)(2L+1)(2S+1)(2\mathcal{L}+1)(2J_0+1)}$$

$$\times \begin{Bmatrix} L_1 & S_1 & J_1 \\ \mathcal{L} & S_0 & j \\ L & S & J \end{Bmatrix} \begin{Bmatrix} \Lambda & L_0 & \mathcal{L} \\ S_0 & j & J_0 \end{Bmatrix} \sum_{M_{T_1},M_{T_0}} (T_1M_{T_1},T_0M_{T_0}|TM_T)$$

$$\times \sum_{M_{L_0},M_{S_0},M_{J_0},M_\Lambda,m_j,M_{J_1}} (L_0M_{L_0},S_0M_{S_0}|J_0M_{J_0})(J_1M_{J_1},jm_j|JM_J)$$

$$\times (\Lambda M_\Lambda,J_0M_{J_0}|jm_j)\,|n\Lambda M_\Lambda\rangle\,|A_1N_1[f_1]L_1S_1T_1J_1:M_{J_1},M_{T_1}\rangle$$

$$\times |A_0N_0[f_0]L_0S_0T_0:M_{L_0}M_{S_0},M_{T_0}\rangle, \qquad (12)$$

where all quantities labeled by subscript 0 and 1 are related to the cluster A_0 and to the residual nucleus A_1, respectively; N_i (i=0,1) is the number of oscillator quanta per nucleus; N is the number of oscillator quanta for the target A; $n = N - N_1 - N_0$ and $\mathbf{\Lambda}$ are quantum numbers of the relative motion wave function (the number of oscillator quanta and orbital angular momentum, correspondingly). In (12) we used the following angular momentum coupling scheme: $\mathbf{T_1} + \mathbf{T_0} = \mathbf{T}$; $\mathbf{L_0} + \mathbf{S_0} = \mathbf{J_0}$, $\mathbf{\Lambda} + \mathbf{J_0} = \mathbf{j}$, $\mathbf{J_1} + \mathbf{j} = \mathbf{J}$. The intrinsic wave functions of the α - cluster (A_0) and the residual nucleus (A_1) depend on corresponding Jacobi coordinates and the relative motion wave function $|n\Lambda M_\Lambda\rangle$ depends on the relative coordinate $\mathbf{R} = \mathbf{R^{A_1}_{c.m.}} - \mathbf{R^{A_0}_{c.m.}}$. The coefficients

$$\langle AN[f]LST|A_1N_1[f_1]L_1S_1T_1;n\Lambda,A_0N_0[f_0]L_0S_0T_0\{\mathcal{L}\}\rangle$$

are the fpc for the separation of four particles from A nucleons of the target nucleus. The fpc can be calculated in the translationally invariant shell model (TISM) [13]. The method

of calculation of these coefficients from the usual shell model fpc [13] is described in Refs. [33,10,16], and the majority of these fpc were tabulated in [17]. The remaining factors in (12) are the standard $6j$-, $9j$- symbols and Clebsch - Gordan coefficients.

D. Matrix element of Coulomb interaction

The final state wave function for the nuclear system (the α - cluster plus the residual nucleus) in the plane wave approximation (PWA) is

$$|f\rangle = \hat{\mathcal{A}}\{e^{i\boldsymbol{P}_1\cdot\boldsymbol{R}^{A_1}_{c.m.}}\mathcal{F}^{A_1}e^{i\boldsymbol{p}'\cdot\boldsymbol{R}^{A_0}_{c.m.}}|A_0N_0[f_0]L_0S_0J_0T_0:M_{J_0}M_{T_0}\rangle\}, \tag{13}$$

where $\hat{\mathcal{A}}$ is the antisymmetrization operator which can be removed from the matrix element due to the antisymmetry of the initial nuclear wave function and symmetry of the electromagnetic interaction operator with respect to particle permutations. As a result, we obtain the combinatorial factor $(A!/A_0!(A-A_0)!)^{1/2}$. The exponential factor $\exp(i\mathbf{P_{final}}\cdot\mathbf{R_{c.m.}})$ describing the center-of-mass motion of the whole nuclear system has already been taken into account during the derivation of the differential cross section (the δ - function of momenta in Eq. (6)). $\mathcal{F}^{A_1}$ is the internal wave function of the residual nucleus which can be written [31] in the intermediate coupling scheme as

$$\mathcal{F}^{A_1} = \sum_{\{[f_{A_1}],L_{A_1},S_{A_1}\}} a^{A_1,J_{A_1}T_{A_1}}_{[f_{A_1}]L_{A_1}S_{A_1}}|A_1N_{A_1}[f_{A_1}]L_{A_1}S_{A_1}J_{A_1}T_{A_1}:M_{J_{A_1}}M_{T_{A_1}}\rangle. \tag{14}$$

Then the matrix element for the Coulomb part of electromagnetic interaction becomes

$$\begin{aligned}\rho_{fi}(\mathbf{q}) = (A!/A_0!(A-A_0)!)^{1/2} &\sum_{\{[f],L,S\}} a^{A,JT}_{[f]LS}\sum_{\{[f_1],L_1,S_1\}} a^{A_1,J_1T_1}_{[f_1]L_1S_1}\sum_{N_0,[f_0],L_0,S_0,T_0,J_0,\Lambda,\mathcal{L},j,n}\\
&\times\langle AN[f]LST|A_1N_1[f_1]L_1S_1T_1;n\Lambda,A_0N_0[f_0]L_0S_0T_0\{\mathcal{L}\}\rangle(-1)^{\Lambda+L_0+j+S_0}\\
&\times\sqrt{(2J_1+1)(2j+1)(2L+1)(2S+1)(2\mathcal{L}+1)(2J_0+1)}\begin{Bmatrix}\Lambda & L_0 & \mathcal{L}\\ S_0 & j & J_0\end{Bmatrix}\\
&\times\begin{Bmatrix}L_1 & S_1 & J_1\\ \mathcal{L} & S_0 & j\\ L & S & J\end{Bmatrix}\sum_{M_{T_1},M_{T_0}}(T_1M_{T_1},T_0M_{T_0}|TM_T)\sum_{M_{J_1},M_{J_0},M_\Lambda,M_j}\end{aligned}$$

$$\times (\Lambda M_\Lambda, J_0 M_{J_0}|jM_j)(J_1 M_{J_1}, jM_j|JM_J)$$
$$\times \langle e^{i\mathbf{R}\cdot\mathbf{P_1}}|e^{-(2i/3)\mathbf{R}\cdot\mathbf{q}}|n\Lambda M_\Lambda\rangle \rho^\alpha_{fi}(\mathbf{q}). \qquad (15)$$

The quantum numbers of the residual nucleus A_1: N_1, $[f_1]$, L_1, S_1, J_1, T_1, M_{J_1}, M_{T_1} are fixed by the experimental conditions which select definite final states. The appearance of the additional factor $\exp[-(2i/3)\mathbf{R}\cdot\boldsymbol{q}]$ in the matrix element for the relative motion part of the wave function is due to the transformation from the center-of-mass of the whole nuclear system to the two-center system of the α-cluster plus the residual nucleus. In Eq. (15) $\rho^\alpha_{fi}(\mathbf{q})$ is the matrix element of the Coulomb interaction of the electron with the nucleons of the knocked out α-cluster.

The experiment detects a free α-particle with the ground state quantum numbers $|\alpha_0\rangle \equiv |A_0 N_0[f_0] L_0 S_0 J_0 T_0 : M_{J_0} M_{T_0}\rangle = |40[4]0000 : 00\rangle$, and the corresponding matrix element can be easily calculated. Using again the fractional parentage technique and separating a single nucleon from the wave functions of the α-cluster, we obtain

$$\rho^\alpha_{fi}(\mathbf{q}) \equiv \langle\alpha_0| \int e^{i\mathbf{q}\cdot\mathbf{r}}\hat{\rho}(\mathbf{r})\mathbf{dr}|\mathbf{4N_0[f_0]L_0S_0J_0T_0 : M_{J_0}M_{T_0}}\rangle$$
$$= 4 \sum_{M_{L_0}, M_{S_0}} \langle 000|e^{-(3i/4)\mathbf{q}\cdot\mathbf{x}}|N_0 L_0 M_{L_0}\rangle (L_0 M_{L_0}, S_0 M_{S_0}|J_0 M_{J_0})$$
$$\times \sum_{S_3, T_3} \langle 40[4]000|30[3]0 S_3 T_3, 00\rangle \langle 4N_0[f_0] L_0 S_0 T_0|30[3]0 S_3 T_3, N_0 L_0\rangle$$
$$\times \sum_{M_{T_3}, m_t, m'_t} (T_3 M_{T_3}, \frac{1}{2} m_t|T_0 M_{T_0})(T_3 M_{T_3}, \frac{1}{2} m'_t|00)\langle \frac{1}{2} m'_t|\frac{e}{2}(1+\tau_3(4))|\frac{1}{2} m_t\rangle, \qquad (16)$$

since the Coulomb interaction is diagonal with respect to spin variables. The particular values $\langle 4N_0[f_0]L_0S_00|30[3]0S_3T_3, N_0L_0\rangle$ of the one particle fpc in TISM are tabulated in [32]. The orbital matrix element for the separated nucleon is calculated by means of decomposition of the exponential function in a spherical harmonic series. After some algebra, one obtains

$$\langle 000|e^{-(3i/4)\mathbf{q}\cdot\mathbf{x}}|N_0 L_0 M_{L_0}\rangle = \sqrt{4\pi} i^{-L_0} Y_{L_0 M_{L_0}}(\mathbf{q}) \int_0^\infty \mathbf{j_{L_0}}\left(\frac{\mathbf{3}}{\mathbf{4}}\mathbf{qx}\right) \mathbf{\Phi_{00}(x)\Phi_{N_0L_0}(x)x^2\,dx}. \quad (17)$$

Here $\Phi_{N_0 L_0}(x)$ is the radial part of the separated nucleon wave function which was taken as that of the harmonic oscillator. For brevity we introduce below the notation $I_{N_0 L_0}(q)$ for the integral in (17). The actual argument in the oscillator functions $\Phi_{N_0 L_0}$ is x/x_0, where x_0

is the oscillator radius of the separated nucleon with the corresponding Jacobi coordinate x. In all calculations the value x_0=1.3 fm had been used [34] determined from the elastic electron scattering data for the ^{4}He nucleus.

The isospin part of the matrix element (16) is defined by the particular isospin value of the residual nucleus ($\mathbf{T_1}+\mathbf{T_0}=\mathbf{0}$) and in the case of the isospin-diagonal transition ^{12}C($T=0$) $\rightarrow^8$Be($T=0$) is equal to unity. For a diagonal transition, the intrinsic wave function of the cluster retains its spatial symmetry in the process of electromagnetic interaction which is equivalent to the conservation of the Young tableaux $[f_0]=[4]$. We have here a nearly complete formal analogy with the case of nucleon - α low energy scattering, the case considered in Ref. [17]. The structure of the matrix element is the same except for minor details. Finally, the transition charge density to be used in Eq. (15) can be written as

$$\rho^{\alpha}_{fi}(\mathbf{q}) = 2e\sqrt{4\pi}\langle 4N_0[f_0]L_000|30[3]0\frac{1}{2}\frac{1}{2}, N_0L_0\rangle\langle 40[4]000|30[3]0\frac{1}{2}\frac{1}{2}, 00\rangle$$
$$\times\, i^{-L_0}Y_{L_0M_{L_0}}(\Omega_q)I_{N_0L_0}(q). \qquad (18)$$

The relative motion part of the matrix element is calculated similarly to (17)

$$\langle e^{i\mathbf{R}\cdot\mathbf{P_1}}|e^{-(2i/3)\mathbf{R}\cdot\mathbf{q}}|n\Lambda M_\Lambda\rangle = 4\pi i^{-\Lambda}Y_{\Lambda M_\Lambda}(\Omega_{P_1})J_{n\Lambda}(P_1), \qquad (19)$$

where the integral $J_{n\Lambda}(P_1)\equiv\int_0^\infty j_\Lambda(P_1R)\Phi_{n\Lambda}(R)R^2\,dR$ gives the effective momentum distribution of the residual nucleus or, equivalently, of the knocked out α - cluster inside the target nucleus. In the absence of the dynamical rebuilding of the cluster, $J_{40}(P_{A_1})$ would be the usual momentum distribution which is determined in the traditional (e,e'α) experiments.

Taking into account (19) we can rewrite the matrix element (15) in the form

$$\rho_{fi}(\mathbf{q}) = 2e(4\pi)^{3/2}\left(\begin{array}{c}A\\ \\ A_0\end{array}\right)^{1/2}\sum_{\{[f],L,S\}}a^{A,JT}_{[f]LS}\sum_{\{[f_1],L_1,S_1\}}a^{A_1,J_1T_1}_{[f_1]L_1S_1}\sum_{N_0,[f_0],L_0,S_0,T_0,J_0,\Lambda,\mathcal{L},j,n}$$
$$\times\,\langle AN[f]LST|A_1N_1[f_1]L_1S_1T_1;n\Lambda,A_0N_0[f_0]L_0S_0T_0\{\mathcal{L}\}\rangle(-1)^{\Lambda+L_0+j+S_0}$$
$$\times\,\sqrt{(2J_1+1)(2j+1)(2L+1)(2S+1)(2\mathcal{L}+1)(2J_0+1)}\left\{\begin{array}{ccc}\Lambda & L_0 & \mathcal{L}\\ \\ S_0 & j & J_0\end{array}\right\}$$

$$\times \left\{ \begin{array}{ccc} L_1 & S_1 & J_1 \\ \mathcal{L} & S_0 & j \\ L & S & J \end{array} \right\} \langle 4N_0[f_0]L_0 00|30[3]0\frac{1}{2}\frac{1}{2}, N_0L_0\rangle \langle 40[4]000|30[3]0\frac{1}{2}\frac{1}{2}, 00\rangle$$

$$\times i^{-\Lambda-L_0} J_{n\Lambda}(P_1) I_{N_0L_0}(q) \sum_{M_{J_0},M_\Lambda,M_j} (\Lambda M_\Lambda, J_0 M_{J_0}|jM_j)(J_1 M_{J_1}, jM_j|JM_J)$$

$$\times Y_{\Lambda M_\Lambda}(\Omega_{P_1}) Y_{L_0 M_{L_0}}(\Omega_q). \qquad (20)$$

This is the general expression for the matrix element of quasielastic knock-out of the α - particle from any p-shell nucleus with isospin $T = 0$ provided that the residual nucleus has zero isospin ($T_1 = 0$) too. A further simplification is possible for particular values of the total angular momentum of the target nucleus J. In the case of the reaction ^{12}C(e,e'α)^{8}Be, J_1=0, and, using the specific values of $6j-$ and $9j-$ symbols [35], we obtain

$$\rho_{fi}(\mathbf{q}) = 2e(4\pi)^{3/2} \left(\begin{array}{c} 12 \\ 4 \end{array} \right)^{1/2} \sum_{\{[f],L,L\}} a^{12,00}_{[f]LL} \sum_{\{[f_1],L_1,L\}} a^{8,J_1 0}_{[f_1]L_1 L} \sum_{N_0,L_0,\Lambda} \frac{1}{\sqrt{(2J_1+1)}}$$

$$\times (-1)^{L_1+L} i^{-\Lambda-L_0} \langle 12\,8[f]LL0|8\,4[f_1]L_1L0; 4 - N_0\Lambda, 4N_0[4]L_0 00\{J_1\}\rangle$$

$$\times \langle 4N_0[4]L_0 00|30[3]0\frac{1}{2}\frac{1}{2}, N_0L_0\rangle \langle 40[4]000|30[3]0\frac{1}{2}\frac{1}{2}, 00\rangle J_{n\Lambda}(P_1)$$

$$\times I_{N_0L_0}(q) \sum_{M_{L_0},M_\Lambda} (\Lambda M_\Lambda, L_0 M_{L_0}|J_1 - M_{J_1}) Y_{\Lambda M_\Lambda}(\Omega_{P_1}) Y_{L_0 M_{L_0}}(\Omega_q). \qquad (21)$$

The differential cross section (9) involves the absolute value of the matrix element squared and summed over the angular momentum projections of the residual nucleus,

$$\sum_{M_{J_1}} \rho_{fi}(\mathbf{q}) \rho^*_{\mathrm{fi}}(\mathbf{q}) = 16\pi e^2 \left(\begin{array}{c} 12 \\ 4 \end{array} \right)^{1/2} \sum_{\{[f],L,L\}} \sum_{\{[f'],L',L'\}} \sum_{\{[f_1],L_1,L\}} \sum_{\{[f_1'],L_1',L'\}} a^{12,00}_{[f]LL} a^{12,00}_{[f']L'L'}$$

$$\times a^{8,J_1 0}_{[f_1]L_1 L} a^{8,J_1 0}_{[f_1']L_1'L'} \sum_{N_0,N_0',L_0,L_0',\Lambda,\Lambda'} (-1)^{L_1+L+L_0+L_1'+L'+L_0'+J_1} i^{-\Lambda-L_0+\Lambda'+L_0'}$$

$$\times \langle 12\,8[f]LL0|8\,4[f_1]L_1L0; 4 - N_0\Lambda, 4N_0[4]L_0 00\{J_1\}\rangle$$

$$\times \langle 12\,8[f']L'L'0|8\,4[f_1']L_1'L'0; 4 - N_0'\Lambda', 4N_0'[4]L_0' 00\{J_1\}\rangle$$

$$\times \langle 4N_0[4]L_0 00|30[3]0\frac{1}{2}\frac{1}{2}, N_0L_0\rangle \langle 4N_0'[4]L_0' 00|30[3]0\frac{1}{2}\frac{1}{2}, N_0'L_0'\rangle$$

$$\times \langle 40[4]000|30[3]0\frac{1}{2}\frac{1}{2}, 00\rangle^2 \sqrt{(2\Lambda+1)(2\Lambda'+1)(2L_0+1)(2L_0'+1)}$$

$$\times J_{n\Lambda}(P_1) J_{n'\Lambda'}(P_1) I_{N_0L_0}(q) I_{N_0'L_0'}(q) \sum_{l=|L_0-L_0'|}^{L_0+L_0'} (\Lambda 0, \Lambda' 0|l0)$$

$$\times (L_0 0, L_0' 0 | l 0) \left\{ \begin{array}{ccc} L_0 & \Lambda & J_1 \\ \Lambda' & L_0' & l \end{array} \right\} P_l(\cos(\widehat{\mathbf{q}, \mathbf{P}_1})). \quad (22)$$

Changing the particular values of the fpc for the separation of four particles from the target nucleus, we can adjust this expression for the description of any reaction ($J_A = 0$, $T_A = 0$) $\rightarrow$ ($J_{A_1} = 0$, $T_{A_1} = 0$), for example ^{16}O(e,e'α)^{12}C.

In contrast to traditional approaches, Eq. (22) exactly accounts for all cluster transition amplitudes allowed by conservation laws and selection rules. The diagonal amplitude with respect to the intrinsic state of the cluster and the amplitudes describing the rebuilding of the orbital part of its wave function appear on equal footing. Thus, for the transition into the ground state $J^\pi = 0^+$ of the residual nucleus ^{8}Be, the diagonal amplitude is the one with the quantum numbers $N_0 = 0$, $L_0 = 0$, $n = 4$ and $\Lambda = 0$, and the nondiagonal amplitudes are those with the following sets of quantum numbers: 2,0,2,0; 2,2,2,2; 3,1,1,1 and 4,0,0,0. In the transition into the first excited state $J^\pi = 2^+$ of ^{8}Be (the excitation energy $E_x \approx 2.9$ MeV), the diagonal amplitude has quantum numbers 0,0,2,2, whereas there are six nondiagonal amplitudes: 2,0,2,2; 2,2,2,0; 2,2,2,2; 3,1,1,1; 3,3,1,1, and 4,2,0,0. The second excited state $J^\pi = 4^+$ ($E_x \approx 11.4$ MeV) is characterized by the diagonal amplitude 4,4,0,0 and nondiagonal ones 3,3,1,1; 2,2,2,2 and 0,0,4,4. All amplitudes, diagonal and nondiagonal, are calculated with their specific wave functions of the knocked out α - cluster and the residual ^{8}Be nucleus in the target nucleus ^{12}C and different sets of quantum numbers n and Λ. The existence of a large amount of interfering amplitudes puts limitations on the possibility of extraction of the momentum distribution of the residual nucleus in such experiments.

III. FINAL STATE INTERACTION EFFECTS

Here we discuss modifications of the basic formalism caused by the distortion in the exit reaction channel. The simplest way of including the final state interaction between the knocked out cluster and the residual nucleus is the standard DWIA approach. The wave

function of the nuclear system (α plus ^{8}Be) in the final state is

$$|f\rangle = \hat{\mathcal{A}}\{e^{i\mathbf{P_{final}}\cdot\mathbf{R_{c.m.}}}\mathcal{F}^{A_1}\chi^{(-)}(\mathbf{p_{rel}},\mathbf{R})|\mathbf{A_0N_0[f_0]L_0S_0J_0T_0}:\mathbf{M_{J_0}M_{T_0}}\rangle\}. \tag{23}$$

Here $\chi^{(-)}(\mathbf{p_{rel}},\mathbf{R})$ is the wave function of the relative motion of the α - cluster and the residual nucleus with asymptotics of an outgoing spherical wave; $p_{rel} = (A_0/A)\mathbf{P_1} - (\mathbf{A_1/A})\mathbf{p'}$ is the momentum associated with the corresponding coordinate $\mathbf{R}$. After same algebra we obtain the matrix element for the Coulomb part of electromagnetic interaction which is similar to that for the PWIA case (15) but the relative motion part in the last line of Eq. (15) is replaced by

$$\langle\chi^{(-)}(\mathbf{p_{rel}},\mathbf{R})|\mathbf{e^{-(2i/3)R\cdot q}}|\mathbf{n\Lambda M_\Lambda}\rangle. \tag{24}$$

The calculation can be performed with the help of the partial wave expansion of the relative motion function

$$\chi^{(-)}(\mathbf{p_{rel}},\mathbf{R}) = 4\pi\sum_{\mathbf{l_1}=0}^{\infty}\sum_{\mathbf{M_{l_1}}=-\mathbf{l_1}}^{\mathbf{l_1}}\mathbf{i^{l_1}}\chi_{\mathbf{l_1}}(\mathbf{p_{rel}},\mathbf{R})\mathbf{Y_{l_1M_{l_1}}}(\mathbf{\Omega_R})\mathbf{Y^*_{l_1M_{l_1}}}(\mathbf{\Omega_{p_{rel}}}), \tag{25}$$

and of the exponent

$$e^{-(2i/3)\mathbf{R}\cdot\mathbf{q}} = 4\pi\sum_{l_2=0}^{\infty}\sum_{M_{l_2}=-l_2}^{l_2}(-i)^{l_2}j_{l_2}\left(\frac{2}{3}qR\right)Y^*_{l_2M_{l_2}}(\Omega_R)Y_{l_2M_{l_2}}(\Omega_q). \tag{26}$$

After the integration over the angular arguments, we obtain

$$\begin{aligned}\langle\chi^{(-)}(\mathbf{p_{rel}},\mathbf{R})|\mathbf{e^{-(2i/3)R\cdot q}}|\mathbf{n\Lambda M_\Lambda}\rangle = (4\pi)^{3/2}&\sum_{l_1,l_2=0}^{\infty}\sum_{M_{l_1},M_{l_2}}(-i)^{l_1+l_2}(-1)^{l_1+l_2-\Lambda}\\ &\times\sqrt{\frac{(2l_1+1)(2l_2+1)}{2\Lambda+1}}(l_10,l_20|\Lambda0)(l_1M_{l_1},l_2M_{l_2}|\Lambda M_\Lambda)\\ &\times J_{l_1l_2n\Lambda}(p_{rel},q)Y_{l_1M_{l_1}}(\Omega_{p_{rel}})Y_{l_2M_{l_2}}(\Omega_q),\end{aligned} \tag{27}$$

where

$$J_{l_1l_2n\Lambda}(p_{rel},q) = \int_0^\infty\chi^{(-)*}_{l_1}(p_{rel},R)j_{l_2}(\frac{A_1}{A}qR)\Phi_{n\Lambda}(R)R^2\,dR. \tag{28}$$

Then, after summation over M_Λ, M_{l_2} and M_{L_0} [35], the matrix element of Coulomb interaction becomes, similar to (15),

$$\rho_{fi}(\mathbf{q}) = 6\sqrt{55}e(4\pi)^{3/2} \sum_{\{[f],L,L\}} a^{12,00}_{[f]LL} \sum_{\{[f_1],L_1,L\}} a^{8,J_10}_{[f_1]L_1L} \sum_{N_0,L_0,\Lambda} (-1)^{L_1+L+\Lambda_i-L_0}$$
$$\times \sqrt{\frac{2L_0+1}{2J_1+1}} \langle 12\,8[f]LL0|8\,4[f_1]L_1L0; 4-N_0\Lambda, 4N_0[4]L_000\{J_1\}\rangle$$
$$\times \langle 4N_0[4]L_000|30[3]0\frac{1}{2}\frac{1}{2}, N_0L_0\rangle \langle 40[4]000|30[3]0\frac{1}{2}\frac{1}{2}, 00\rangle I_{N_0L_0}(q)$$
$$\times \sum_{l_1,l_2=0}^{\infty} (2l_2+1)\sqrt{2l_1+1}(l_10, l_20|\Lambda 0) J_{l_1l_2n\Lambda}(p_{rel}, q) \sum_{l_4=|L_0-l_2|}^{L_0+l_2} (L_00, l_20|l_40)$$
$$\times \begin{Bmatrix} J_1 & \Lambda & L_0 \\ l_2 & l_4 & l_1 \end{Bmatrix} \sum_{M_{l_1},M_{l_4}} (-1)^{-M_{J_1}} (l_4M_{l_4}, l_1M_{l_1}|-M_{J_1})$$
$$\times Y_{l_1M_{l_1}}(\Omega_{p_{rel}}) Y_{l_4M_{l_4}}(\Omega_q). \qquad (29)$$

Going over to the $\sum_{M_{J_1}} \rho_{fi}(\mathbf{q})\rho^*_{\mathfrak{fi}}(\mathbf{q})$ as in the case of PWIA approximation and implementing all needed transformations, we obtain ultimately the DWIA analog of PWIA formula (22)

$$\sum_{M_{J_1}} \rho_{fi}(\mathbf{q})\rho^*_{\mathfrak{fi}}(\mathbf{q}) = 7920\pi e^2 \sum_{\{[f],L,L\}} \sum_{\{[f'],L',L'\}} \sum_{\{[f_1],L_1,L\}} \sum_{\{[f'_1],L'_1,L'\}} a^{12,00}_{[f]LL} a^{12,00}_{[f']L'L'}$$
$$\times a^{8,J_10}_{[f_1]L_1L} a^{8,J_10}_{[f'_1]L'_1L'} \sum_{N_0,N'_0,L_0,L'_0,\Lambda,\Lambda'} (-1)^{L_1+L+\Lambda+L'_1+L'+\Lambda'+J_1 i-L_0+L'_0}$$
$$\times \langle 12\,8[f]LL0|8\,4[f_1]L_1L0; 4-N_0\Lambda, 4N_0[4]L_000\{J_1\}\rangle$$
$$\times \langle 12\,8[f']L'L'0|8\,4[f'_1]L'_1L'0; 4-N'_0\Lambda', 4N'_0[4]L'_000\{J_1\}\rangle$$
$$\times \langle 4N_0[4]L_000|30[3]0\frac{1}{2}\frac{1}{2}, N_0L_0\rangle \langle 4N'_0[4]L'_000|30[3]0\frac{1}{2}\frac{1}{2}, N'_0L'_0\rangle$$
$$\times \langle 40[4]000|30[3]0\frac{1}{2}\frac{1}{2}, 00\rangle^2 I_{N_0L_0}(q) I_{N'_0L'_0}(q) \sqrt{(2L_0+1)(2L'_0+1)}$$
$$\times \sum_{l_1,l_2=0}^{\infty} \sum_{l'_1,l'_2=0}^{\infty} i^{l_1+l_2-l'_1-l'_2}(2l_1+1)(2l_2+1)(2l'_1+1)(2l'_2+1)$$
$$\times (l_10, l_20|\Lambda 0)(l'_10, l'_20|\Lambda' 0) J_{l_1l_2n\Lambda}(p_{rel}, q) J^*_{l'_1l'_2n'\Lambda'}(p_{rel}, q)$$
$$\times \sum_{l_4=|L_0-l_2|}^{L_0+l_2} \sum_{l'_4=|L'0-l'_2|}^{L'_0+l'_2} (L_00, l_20|l_40)(L'_00, l'_20|l'_40) \sqrt{(2l_4+1)(2l'_4+1)}$$
$$\times \begin{Bmatrix} J_1 & \Lambda & L_0 \\ l_2 & l_4 & l_1 \end{Bmatrix} \begin{Bmatrix} J_1 & \Lambda' & L'_0 \\ l'_2 & l'_4 & l'_1 \end{Bmatrix} \sum_{\tilde{l}_1=|l_1-l'_1|}^{l_1+l'_1} (l_10, l'_10|\tilde{l}_10)$$
$$\times (l_40, l'_40|\tilde{l}_10)(-1)^{l_1+l'_1} \begin{Bmatrix} l_1 & l_4 & J_1 \\ l'_4 & l'_1 & \tilde{l}_1 \end{Bmatrix} P_{\tilde{l}_1}(\cos(\mathbf{q}, \widehat{\mathbf{p}_{\mathbf{rel}}})). \qquad (30)$$

An essential weak "technological" point of the approach is the necessity to sum up over a

large number of partial waves (formally we have to sum from zero up to infinity over l_1, l_2, l'_1, l'_2 in the final DWIA formula). Although each individual partial wave expansion converges rather rapidly, especially in the quasielastic peak region, we have four coupled summations in eq. (30). Another difficulty is due to the need for an optical potential for the system $\alpha-^8$Be in the wide energy range (from zero up to few hundred MeV). At present we limit ourselves with a preliminary study of the influence of the distortion on the differential cross section, using a schematic optical potential for $\alpha-^8$Be taken from Ref. [4]. The questions of stability of the cross sections under variations of the parameters and their possible energy dependence are not discussed in this work. We intend to consider these problems more carefully for the reaction ^{16}O(e,e'α)^{12}C where the final state optical potentials are well defined.

IV. RESULTS AND DISCUSSION

The differential cross section is experimentally obtained as a function of the scattered electron energy E'_e (energy sharing experiment). Along with that, we also calculated the angular distributions for fixed energy (and momentum transfer) because this might be more informative from the viewpoint of possible signatures of the nondiagonal transition amplitudes.

In our calculations of the overlap integrals, $J_{n\Lambda}(P_1)$, Eq. (19), in the PWIA, and later the similar integrals, $J_{l_1 l_2 n\Lambda}(p_{rel}, q)$ Eq. (28), in the DWIA, we used for the bound $\Phi_{n\Lambda}$ and scattering states of the $\alpha-^8$Be system the corresponding wave functions in the Woods - Saxon potential [4] with the parameters: real part V=−88.9 MeV, R=1.98 fm, a=0.81 fm; imaginary part W=−4.9 MeV, R=6.02 fm, a=0.58 fm; and the Coulomb potential as the field of a uniformly charged sphere with the radius R_{Coul}=2.4 fm. The real part of the potential has the following spectrum of the lowest states

n	0	1	2	2	3	3	4
Λ	0	1	0	2	1	3	0
E (MeV)	-55.60	-41.95	-29.03	-28.60	-16.92	-15.77	-7.363

so that the state $\Phi_{40}(R)$ is associated with the bound state $\alpha-^8$Be as a ground state of the ^{12}C nucleus. The dependence of the overlap integrals $J_{n\Lambda}(P_1)$ and $J_{l_1 l_2 n\Lambda}(p_{rel}, q)$ on scattered electron energy E'_e determines the behavior of the differential cross section of the reaction.

We start the discussion of the differential cross sections of the ^{12}C(e,e'α)^{8}Be reaction with the simplest PWIA approach. For a crude estimate of the relative contribution of different transition amplitudes (diagonal and nondiagonal with respect to the internal structure of the knocked out α - particle), we calculated the reaction cross section according to (22) for each amplitude separately. The results are presented in Fig. 4 for the transition into the ground state 0^+ of the residual nucleus ^{8}Be. Although the diagonal amplitude in general dominates, in certain regions a number of nondiagonal amplitudes are either comparable to or even greater than the diagonal one. This occurs, in particular, in the diffraction minima of the diagonal amplitude. One should keep in mind that this result does not take into account a possible interference of the amplitudes and therefore provides merely a qualitative illustration of different contributions.

The PWIA differential cross section for the ground state 0^+ of ^{8}Be is presented in Fig. 5 (two lower curves). The solid line corresponds to the full cross section where all allowed transition amplitudes (22) are accounted for while the dashed line shows the contribution of the diagonal amplitude only. The maximum difference between the two cross sections is localized in the region of the quasielastic peak and reaches approximately 20-25%. The interference of the transition amplitudes is destructive and effectively reduces the cross section.

In the case of the transition into the first excited state 2^+ of ^{8}Be the pattern is different. As seen from Fig. 6 (two lower curves), here the interference of amplitudes is constructive and enhances the cross section by approximately 15-20% near the quasielastic peak. The peak shifts to lower energies by the excitation energy E_x=2.9 MeV. An even more noticeable effect exceeding 60% is seen for the transition into the second excited state 4^+ of ^{8}Be, see Fig. 7 (two lower curves) ; again the interference is constructive.

Figs. 5-7 show the cross sections for different final states of the residual nucleus calculated

in the DWIA (two upper curves in each figure). The DWIA curves are plotted together with their PWIA analogs. For this reason the scale of the DWIA data was changed (the magnification coefficients are indicated near the corresponding curves). As we mentioned, these results are more of qualitative character but they give an idea about the influence of distortion in the exit channel. The manifestations of the restructuring of the internal structure of the knocked out cluster are generally suppressed by the distortion, at least at relatively low electron energy used in the present work.

It is instructive to observe the changes in the angular distributions for the transitions into various states of the residual nucleus when one moves over the region of the quasielastic peak. These results obtained in the PWIA are presented in Figs. 8-10 for different energies of the scattered electron. The angular distributions of the knocked out α - particles are shown with respect to the direction of the electron beam and, therefore, are asymmetric with respect to 90°. The recalculation to the direction of the momentum transfer leads to the shift of the angular distribution through a constant angle between the momentum transfer and the electron beam and restores the symmetry. The remarkable feature of the results is the sharp sensitivity of the angular distributions near the quasielastic peak to the missing momentum $\boldsymbol{P}_1 = \boldsymbol{p}' - \boldsymbol{q}$. The whole pattern is very different for different states of the residual nucleus. Form this viewpoint, the presentation in terms of the angular distributions is more revealing than the traditional depicting as a function of the missing momentum. Angular distribution experiments seem to be the most promising for the aim of observing the signatures of nondiagonal processes.

V. CONCLUSION

We have formulated a general microscopic formalism for the description of the quasielastic knock-out of α - clusters by ultrarelativistic electrons from p - shell nuclei. Our major interest was focused on the influence of nuclear structure on the experimentally observed differential cross sections and angular distributions. We have derived all necessary formulas,

including those accounting for the final state interaction between the knocked out cluster and the residual nucleus. Our numerical calculations of the particular ^{12}C(e,e'α)^{8}Be reaction were carried out mainly in the simplest PWIA approximation. The DWIA results bear only qualitative character. The reasons for this are (i) the desire to avoid overloading the formalism by technically complicated details which are of minor importance from the viewpoint of nuclear structure; (ii) the absence of well defined optical potentials for the α - ^{8}Be system. Nevertheless, even at this stage the calculated cross sections and angular distributions allow us to make a number of conclusions.

1. Our consideration shows the importance of the contributions of processes with virtually excited clusters and their subsequent restructuring in the exit channel. We call those contributions "nondiagonal" with respect to the internal state of the knocked out α-cluster. The importance of the virtual processes of this kind was stressed earlier in our study of similar proton-induced knock-out reactions [17].

2. The most appreciably the nondiagonal effects become visible in the vicinity of the quasielastic peak, in particular for the transitions into the excited states of the residual nucleus. For the transitions into 2^+ and 4^+ states of ^{8}Be we have obtained a clear enhancement of the nuclear restructuring effects. The considerable difference of the internal wave functions of the ground state and excited states of the residual nucleus is favorable for the manifestation of the virtually excited cluster components. The different angular momentum coupling schemes in the shell-model wave functions of excited states leads to the constructive interference of various paths of the cluster formation. A fairly poor theoretical description of the ^{12}C(p,p'α)^{8}Be($J^\pi = 2^+$) experimental data in [4] (a hadron analog of our reaction) can, at least partly, be explained by neglecting the nondiagonal effects.

3. The effects due to the final state interaction are in general comparable to the effects caused by the nuclear restructuring. In future comprehensive theory, the distortions in the exit channel are to be fully taken into account, along with all interference

effects. The main problem in this direction is related to the absence of a reliable optical potential for the knocked out cluster interacting with the residual ^{8}Be nucleus. We hope to extend this work to the ^{16}O(e,e'α)^{12}C reaction for which there exist well established optical potentials.

4. In the energy sharing experiments, the observational signatures of the nondiagonal transitions in the cross sections are relatively weak. The influence of virtually excited clusters is quantitative rather than qualitative, at least in the considered electron energy range. This influence is further washed away by the distortion effects.

5. Available experimental data (in plane kinematics) apparently do not allow one to point out clearly the signatures of nuclear restructuring phenomena because of the nonoptimal choice of kinematic conditions. It might be possible to demonstrate nondiagonal effects more clearly by changing the kinematic scheme of the reaction, namely by passing from the plane kinematics to the out-of-plane measurements. Different interfering contributions reveal themselves differently with the arrival of new degrees of freedom. However, since the observables here are determined mainly by the interference between transverse current and Coulomb (plus longitudinal current) components, the effective cross sections and form-factors have considerably lower values. This gives rise to a number of practical dufficulties which increase the demands to the experimental setup. At present, neither theoretical calculations nor experimental data for out-of-plane measurements are available. The formalism presented above can be easily modified in this direction which seems to be a desirable prerequisite for planning the out-of-plane measurements.

6. Angular distribution experiments near the quasielastic peak, especially with polarization observables, seem to be rather promising for disentangling the nondiagonal processes because of the strong sensitivity of the results to the final state of the residual nucleus. The recent technological advances (high duty-factor electron beams and

significant progress in developing polarized targets) give a remarkable opportunity to study polarized electron/target coincidence reactions [19]. Even in the framework of the traditional approaches (without the cluster rebuilding effects), by varying the direction of the target polarization it is possible to decompose each of the response functions into a number of terms involving specific interferences between the multipole matrix elements [36–38]. The use of a polarized electron beam adds more information due to the presence of two extra response functions [36]. The situation looks even more promising when we take into account the restructuring effects due to strong interference between different internal states of the knocked out cluster. The extension of the outlined formalism for the description of polarization phenomena is straightforward and will be the object of following investigations. Our first estimates already reveal the perspectives of such an approach.

7. The comparison, at similar conditions, of the reaction ^{12}C(e,e'α)^{8}Be with its hadron analog ^{12}C(p,p'α)^{8}Be studied earlier [15–17] indicates that, because of the multiple-step character of the interaction of the projectile with the nucleons of the knocked-out cluster in the proton-induced reaction, the momentum distribution of the residual nucleus strongly depends on the orientation angle of its recoil momentum with respect to the initial beam and the proton scattering plane. Such anisotropy is impossible in the case of the single-step interaction, the case of the (e,e'α) scattering, at least in the plane kinematics. Of course, the theoretical calculation for the proton-induced processes is less reliable.

ACKNOWLEDGMENTS

This work was supported by the National Science Foundation, through Grants 95-12831 and 96-05207.

---

[1] A. Arima and S. Kubono, in Treatise on Heavy-Ion Science, edited by D.A. Bromley (Plenum Press, New York, 1984) p. 617.

[2] T.A. Carey et al., Phys. Rev. C **29**, 1273 (1984).

[3] B. Gottschalk and S.L. Kannenberg, Phys. Rev. C **2**, 24 (1970).

[4] P.G. Roos et al., Phys. Rev. C **15**, 69 (1977).

[5] A. Nadasen et al., Phys. Rev. C **22**, 1394 (1980).

[6] C.W. Wang et al., Phys. Rev. C **31**, 1662 (1985).

[7] A. Nadasen et al., Phys. Rev. C **40**, 1130 (1989).

[8] I. Rotter, Nucl. Phys. **A122**, 567 (1968); **A135**, 378 (1969).

[9] R. Bock and H. Yoshida, Nucl. Phys. **A189**, 177 (1972).

[10] V.G. Neudatchin, Yu.F. Smirnov, and N.F. Golovanova, Adv. Nucl. Phys. **11**, 1 (1979).

[11] I.S. Shapiro, in Selected Topics in Nuclear Theory (IAEA, Vienna, 1963) p. 85.

[12] N.S. Chant and P.G. Roos, Phys. Rev. C **15**, 57 (1977).

[13] O.F. Nemets, V.G. Neudatchin, A.T. Rudchik, Yu.F. Smirnov, and Yu.M. Tchuvil'sky, Nucleon Associations in Atomic Nuclei and Nuclear Reactions of Multinucleon Transfer (Naukova Dumka, Kiev, 1988).

[14] N.F. Golovanova et al., Nucl. Phys. **A262**, 444 (1976).

[15] V.G. Neudatchin, A.A. Sakharuk, W.W. Kurovsky, and Yu.M. Tchuvil'sky, Phys. Rev. C **50**, 148 (1994).

[16] Yu.M. Tchuvil'sky, W.W. Kurovsky, A.A. Sakharuk, and V.G.Neudatchin, Phys. Rev. C **51**, 784 (1995).

[17] A.A. Sakharuk and V.G. Zelevinsky, Phys. Rev. C **55**, 302 (1997).

[18] R.J. Glauber, in Lectures in Theoretical Physics (Interscience, New York, 1959) Vol. 1, p. 315.

[19] V.F. Dmitriev et al., Nucl. Phys. **A464**, 237 (1987).

[20] R.G. Satchler, Direct Nuclear Reactions (Clarendon Press, Oxford, 1983).

[21] G. Jacob and A.I.Th. Maris, Nucl. Phys. **31**, 139, 152 (1962); Rev. Mod. Phys. **38**, 121 (1966).

[22] H. Uberall, Electron scattering from complex nuclei (Academic Press, New York, 1971).

[23] C. Ciofi degli Atti, Electron scattering by nuclei (Pergamon Press, Oxford, 1980).

[24] B.L. Berman et al., Phys. Rev. Lett. **62**, 24 (1989); H.J. Mitchell et al., Phys. Rev. C **44**, 2002 (1991).

[25] R. Ent et al., Nucl. Phys. **A 578**, 93 (1994).

[26] Van den Steenhoven, private communication; G. De Meyer, Thesis (Gent, 1997).

[27] A.I. Akhiezer and V.B. Berestetsky, Quantum Electrodynamics (Wiley, New York, 1963).

[28] T. De Forest, Jr. and J.D. Walecka, Adv. Phys. **15**, 1 (1966).

[29] A.I. Akhiezer, A.G. Sitenko, and V.K. Tartakovskii, Nuclear Electrodynamics (Springer-Verlag, Berlin, 1994).

[30] W. Weise, Nucl. Phys. **A193**, 625 (1972).

[31] A.N. Boyarkina, Structure of the p-shell nuclei (Moscow University Press, Moscow, 1973).

[32] V.G. Neudatchin and Yu.F. Smirnov, Nucleon Associations in Light Nuclei (Nauka, Moscow, 1969).

[33] Yu.F. Smirnov and Yu.M. Tchuvil'sky, Phys. Rev. C **15**, 84 (1977).

[34] R.D. Lawson, Theory of the Nuclear Shell Model (Clarendon Press, Oxford, 1980).

[35] A.R. Edmonds, Angular Momentum in Quantum Mechanics (Princeton University Press, Princeton, 1960).

[36] T.W. Donnelly and A.S. Raskin, Ann. Phys. **169**, 247 (1986).

[37] J.A. Caballero, T.W. Donnelly, and G.I. Poulis, Nucl. Phys. **A 555**, 709 (1993).

[38] J.E. Amaro and T.W. Donnelly, Nucl. Phys. **A 646**, 187 (1999).

Figure captions

Figure 1. (a) The kinematic scheme of the reaction ^{12}C(e,e'α)^{8}Be. (b) The Feynman diagram of the reaction ^{12}C(e,e'α)^{8}Be. For the notations see Sec. 2.

Figure 2. Kinematic observables for the reaction ^{12}C(e,e'α)^{8}Be at energy of the initial electron beam E_e=637 MeV, the electron scattering angle θ_e = 26.06° and α - particles registered at 71.08°; solid lines for the transition into the ground state J^π=0$^+$ of ^{8}Be, dashed curves for the transition to the first excited state J^π=2$^+$ (E_x=2.9 MeV), and dash - dotted curves for the second excited state J^π=4$^+$ (E_x=11.4 MeV). (a) Kinetic energy of knocked out α - particles; (b) energy of relative motion of the knocked out α - particle and the residual nucleus; (c) the angle between the momentum of the residual nucleus $\boldsymbol{P}_1$ and the momentum transfer $\boldsymbol{q}$; (d) the angle between $\boldsymbol{p}_{rel}$ and $\boldsymbol{q}$.

Figure 3. The momentum of the residual ^{8}Be nucleus. The notations are the same as in Fig. 2. The minima of the curves correspond to the quasielastic peak.

Figure 4. Relative contributions of different transition amplitudes, diagonal and nondiagonal with respect to the internal structure of the knocked out α-particle, to the calculated reaction cross section for the transition into the ground state 0$^+$ of the residual nucleus ^{8}Be. Contributions of individual amplitudes are shown separately (no interference). The solid line corresponds to the diagonal transition, N_0=0, L_0=0; long-dashed line: N_0=2, L_0=0; short-dashed line: N_0=3, L_0=1; dashed-dotted line: N_0=2, L_0=2; and dotted line: N_0=4, L_0=0.

Figure 5. The differential cross section for the ground state 0$^+$ of ^{8}Be calculated in PWIA (two lower curves) and DWIA (two upper curves). The DWIA data are multiplied by 10^2 times. The solid curves correspond to the full cross section where all allowed transition amplitudes, eq. (22), are accounted for; the dashed curves show the contribution of the diagonal amplitude alone.

Figure 6. The same as Fig. 5 but for the transition into the first excited 2$^+$ state of ^{8}Be. The scaling coefficient is equal to 10.

Figure 7. The same as Fig. 5 but for the transition into the second excited 4^+ state of ^{8}Be.The scaling coefficient is equal to 10.

Figure 8. The α - particle angular distributions for the transition into the ground state of ^{8}Be. The scattered electron energy is 600 MeV (a) and 610 MeV (b). The notations are the same as in Fig. 5.

Figure 9 The same as Fig. 8 but for the transition into the first excited 2^+ state of ^{8}Be.

Figure 10. The same as Fig. 8(a) but for the transition into the second excited 4^+ state of ^{8}Be and the scattered electron energy 580 MeV (a) and 590 MeV (b).

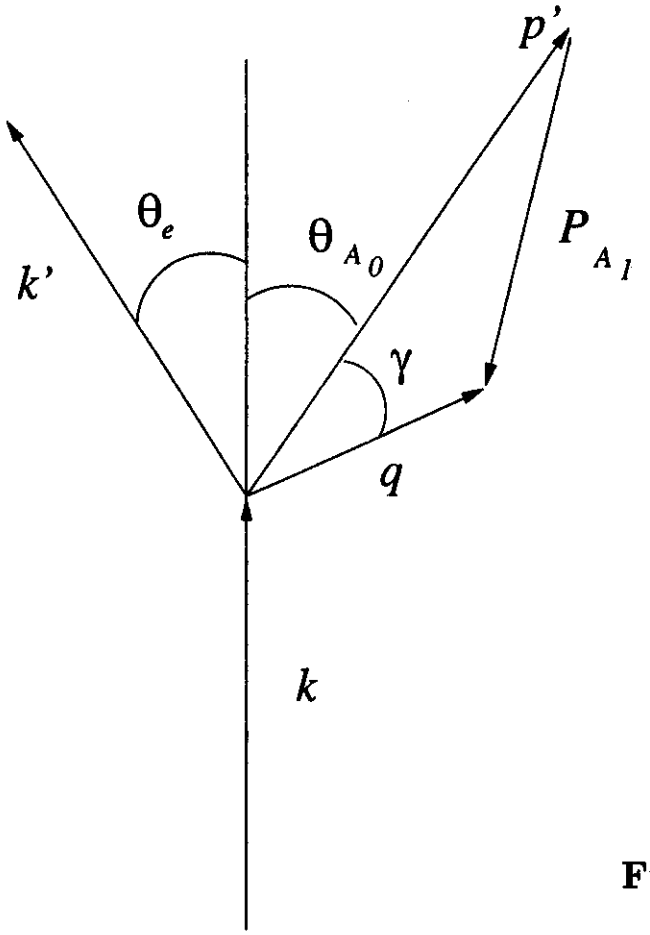

Fig. 1(a)

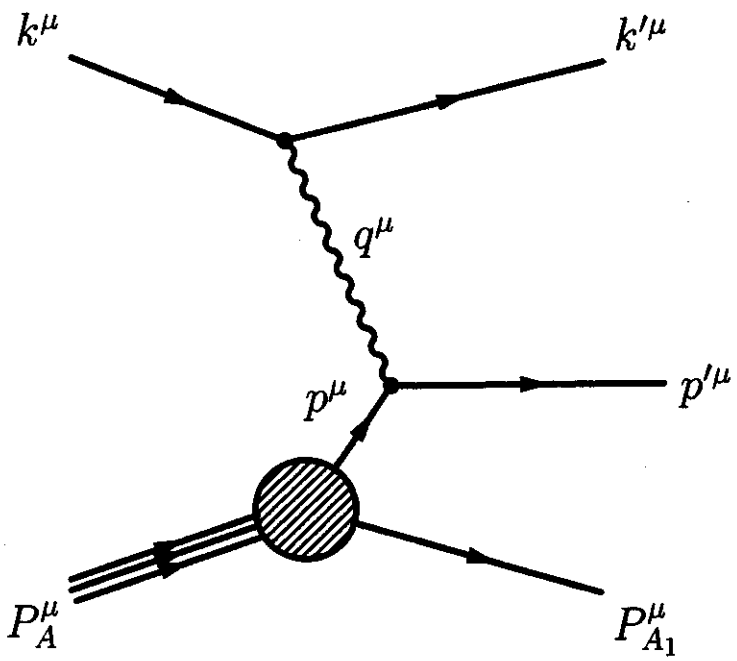

Fig. 1(b)

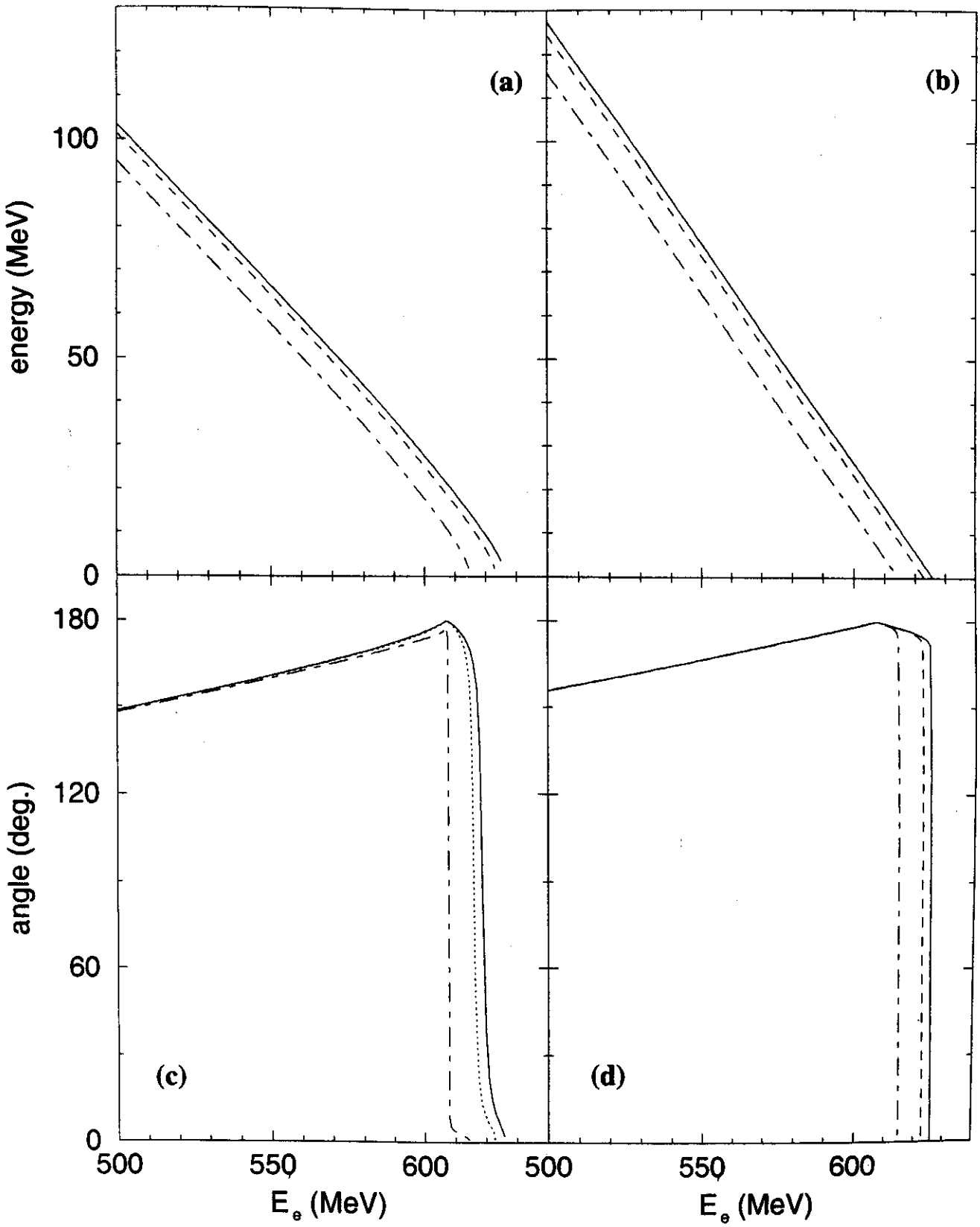
(a)
(b)
(c)
(d)
energy (MeV)
angle (deg.)
100
50
0
180
120
60
0
500
550
600
500
550
600
E_e (MeV)
E_e (MeV)

Fig. 2

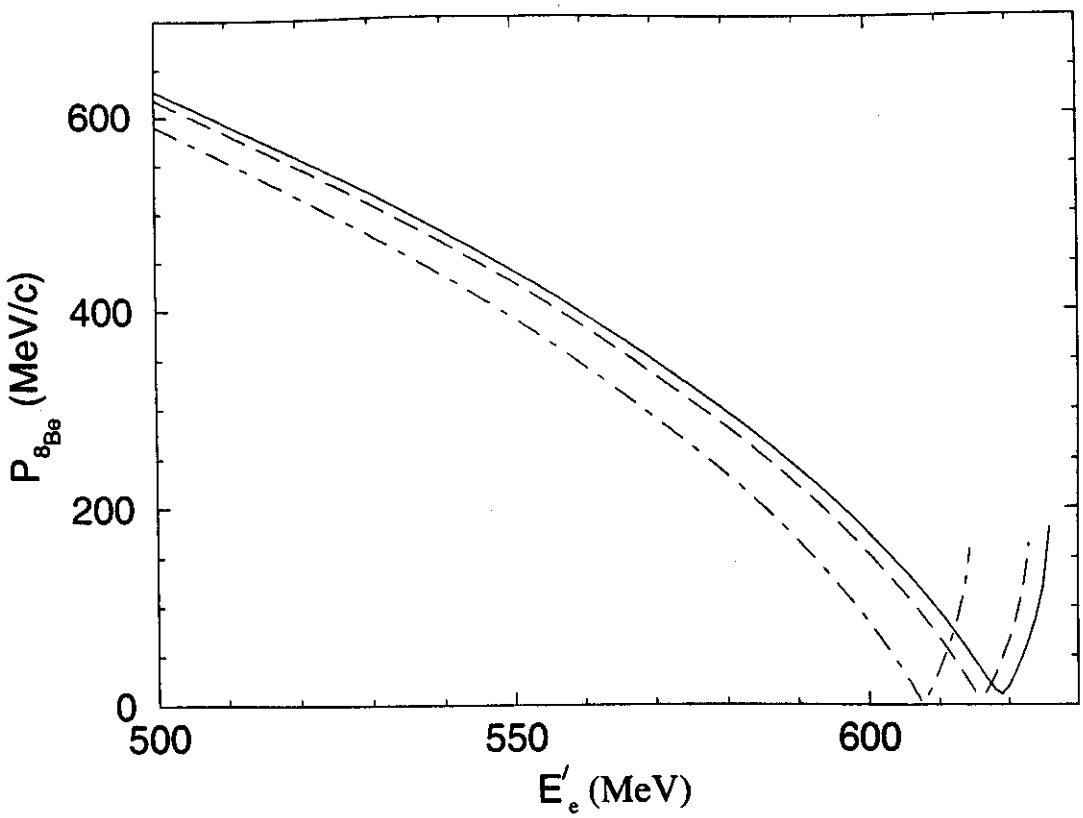
600
400
200
0
500
550
600
$P_{^8Be}$ (MeV/c)
E'_e (MeV)

Fig. 3

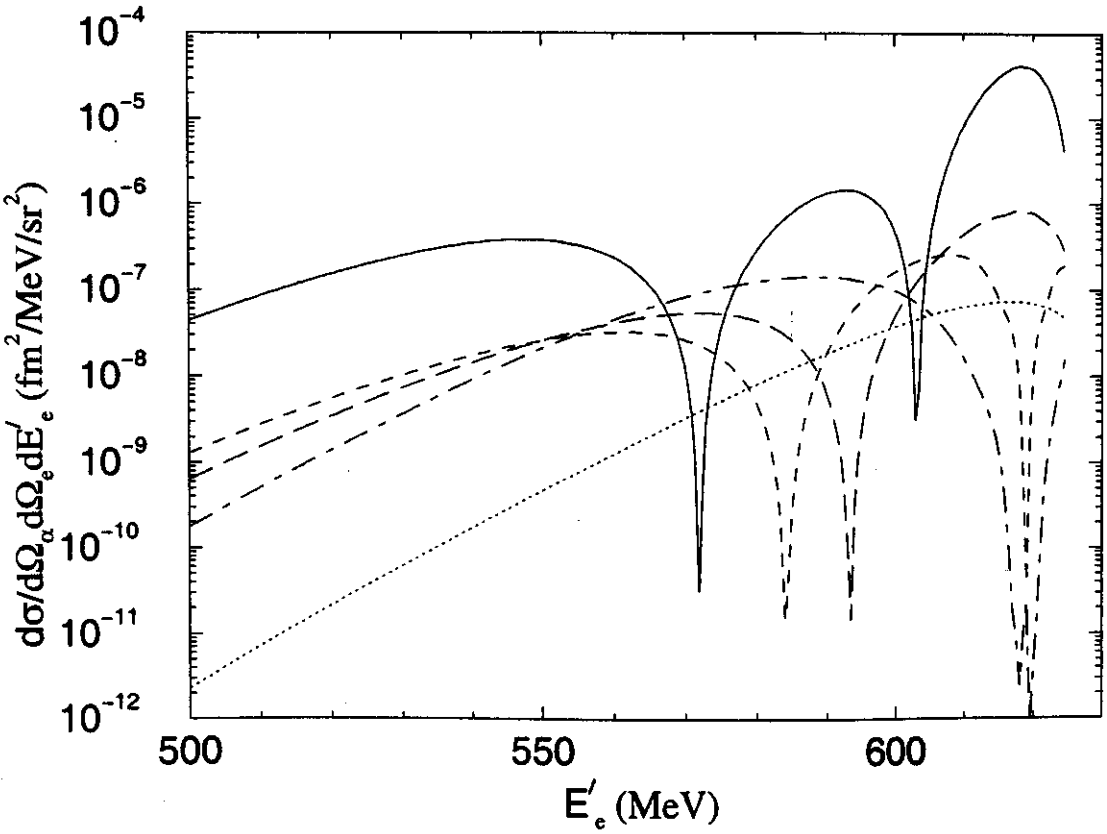
10^{-4}
10^{-5}
10^{-6}
10^{-7}
10^{-8}
10^{-9}
10^{-10}
10^{-11}
10^{-12}
500
550
600
$d\sigma/d\Omega_\alpha d\Omega_e dE'_e$ (fm^2/MeV/sr^2)
E'_e (MeV)

Fig. 4

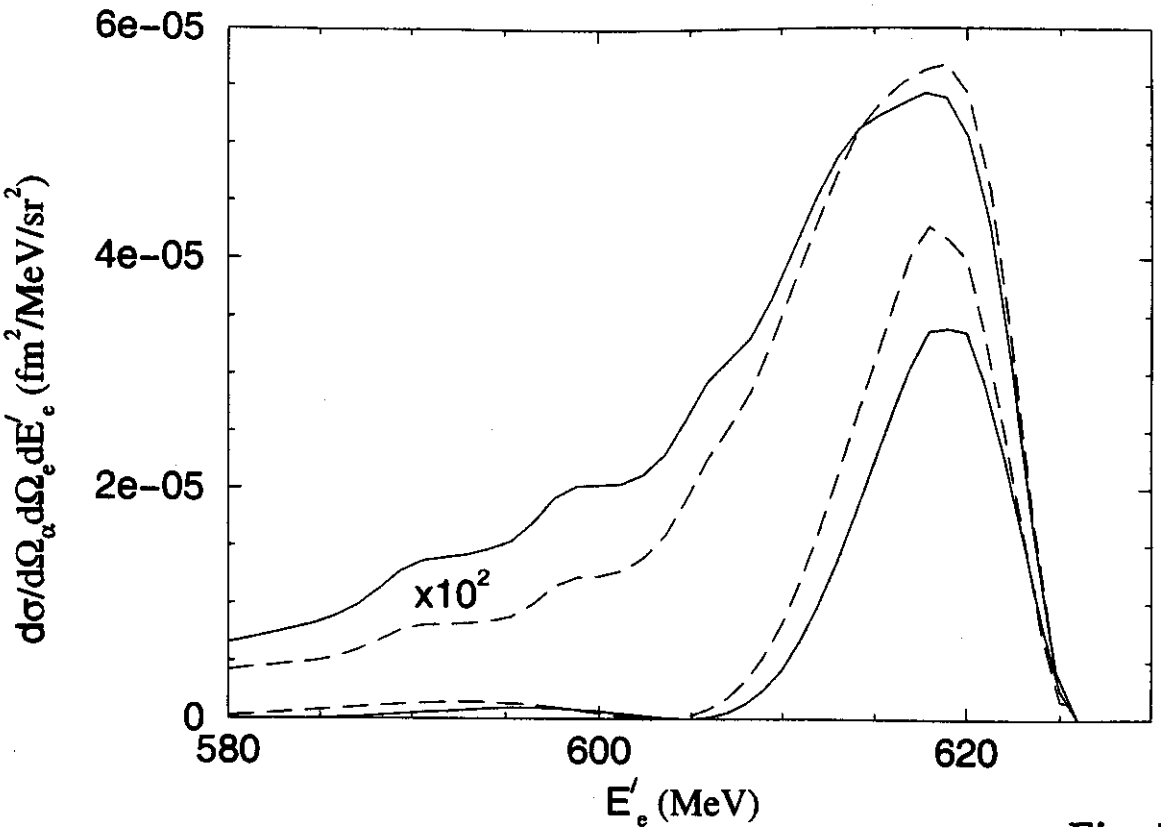
6e-05
4e-05
2e-05
0
580
600
620
x10^2
dσ/dΩ_α dΩ_e dE'_e (fm^2/MeV/sr^2)
E'_e (MeV)

Fig. 5

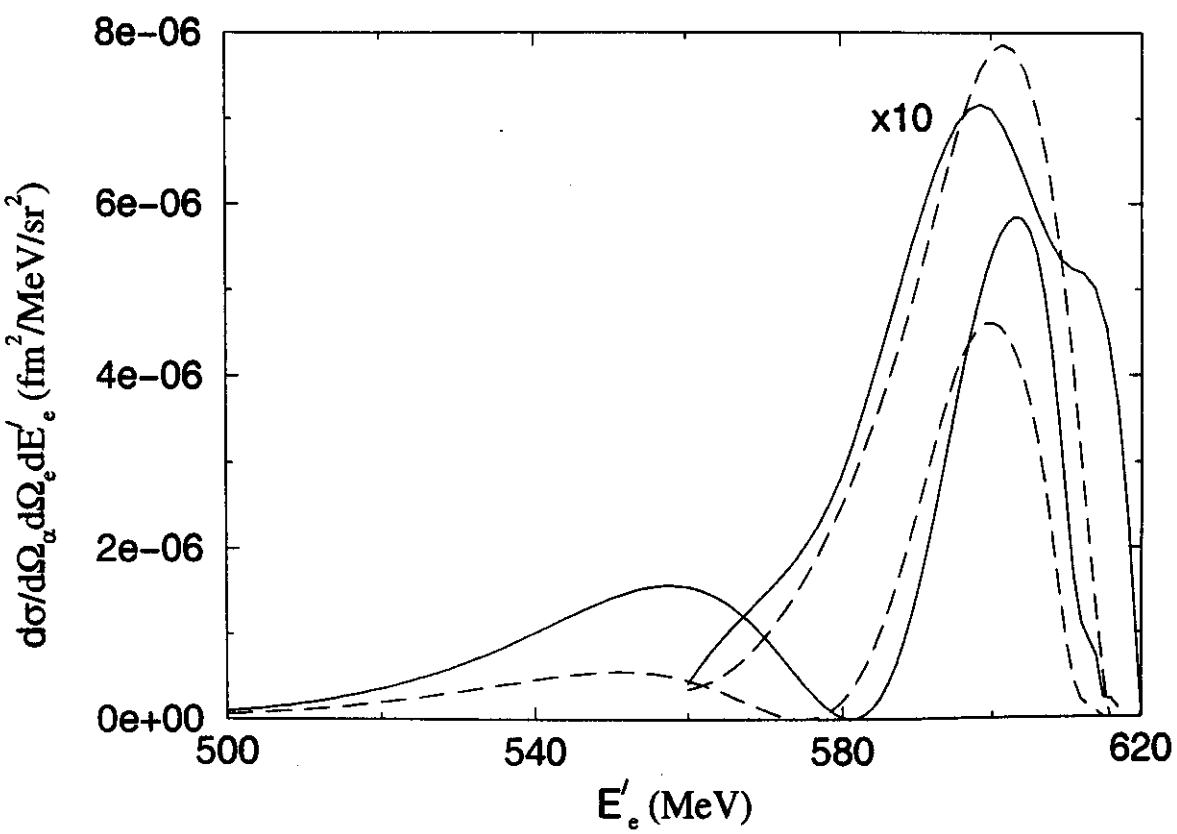
8e-06
6e-06
4e-06
2e-06
0e+00
500
540
580
620
x10
dσ/dΩ_α dΩ_e dE'_e (fm^2/MeV/sr^2)
E'_e (MeV)

Fig. 6

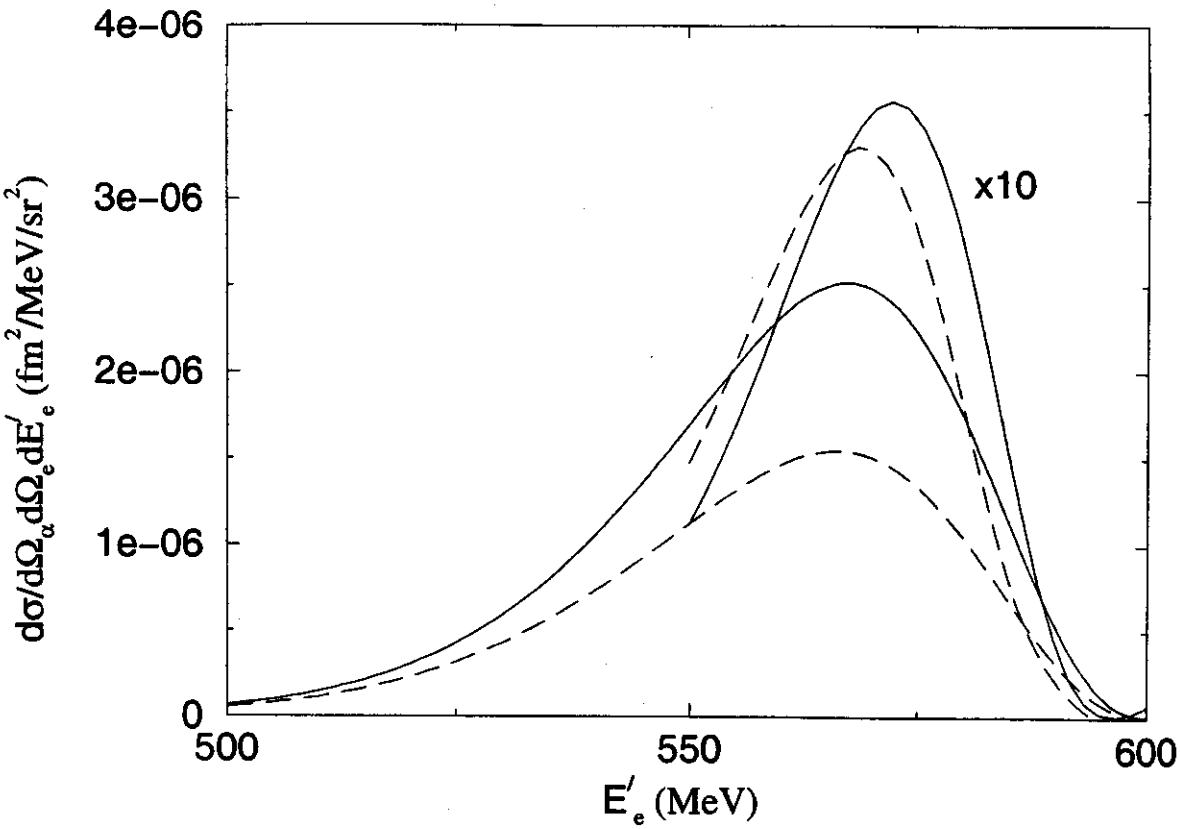
4e-06
3e-06
2e-06
1e-06
0
500
550
600
x10
$d\sigma/d\Omega_\alpha d\Omega_e dE'_e$ (fm^2/MeV/sr^2)
E'_e (MeV)

Fig. 7

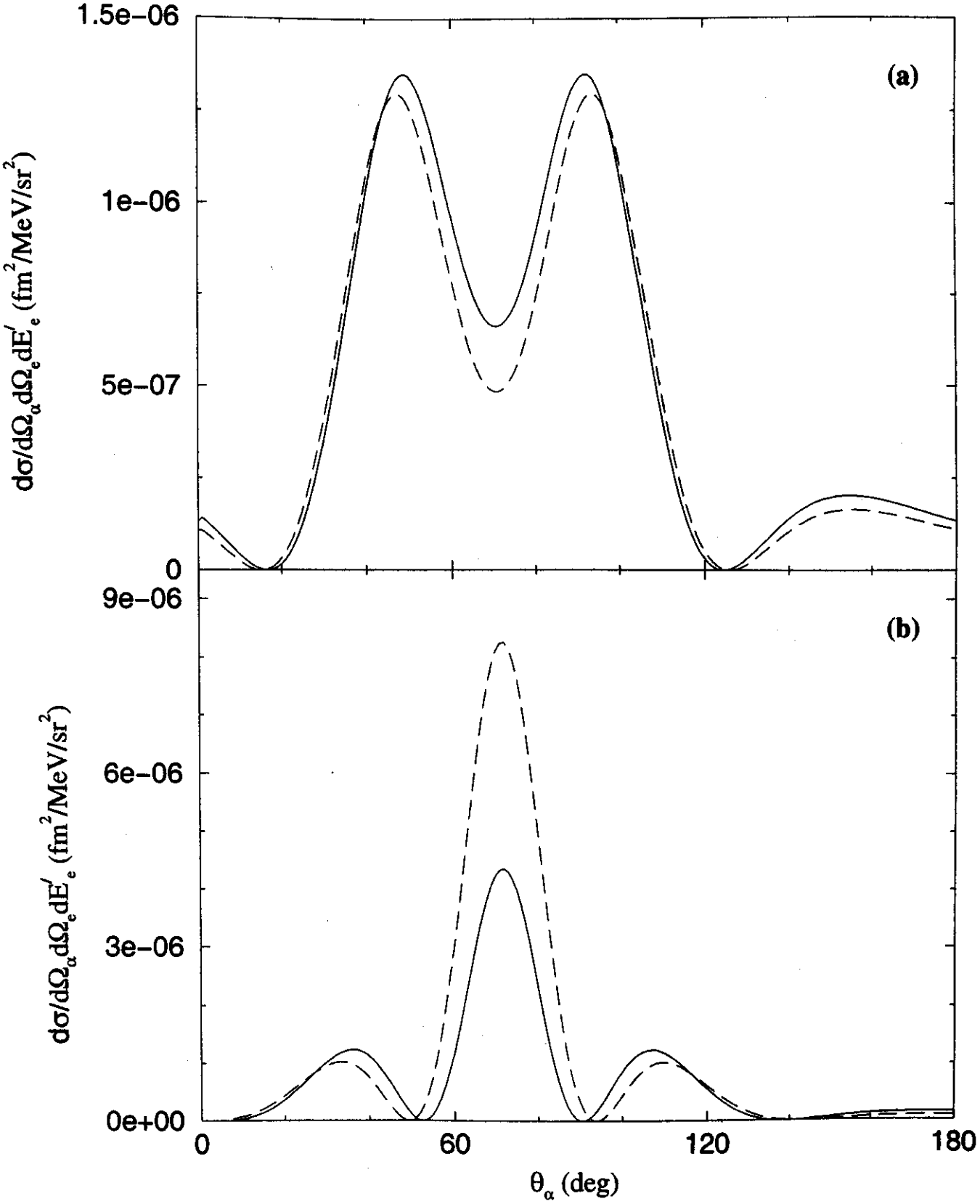
1.5e-06
1e-06
5e-07
0
(a)
dσ/dΩ_α dΩ_e dE'_e (fm²/MeV/sr²)
9e-06
6e-06
3e-06
0e+00
(b)
dσ/dΩ_α dΩ_e dE'_e (fm²/MeV/sr²)
0
60
120
180
θ_α (deg)

Fig. 8

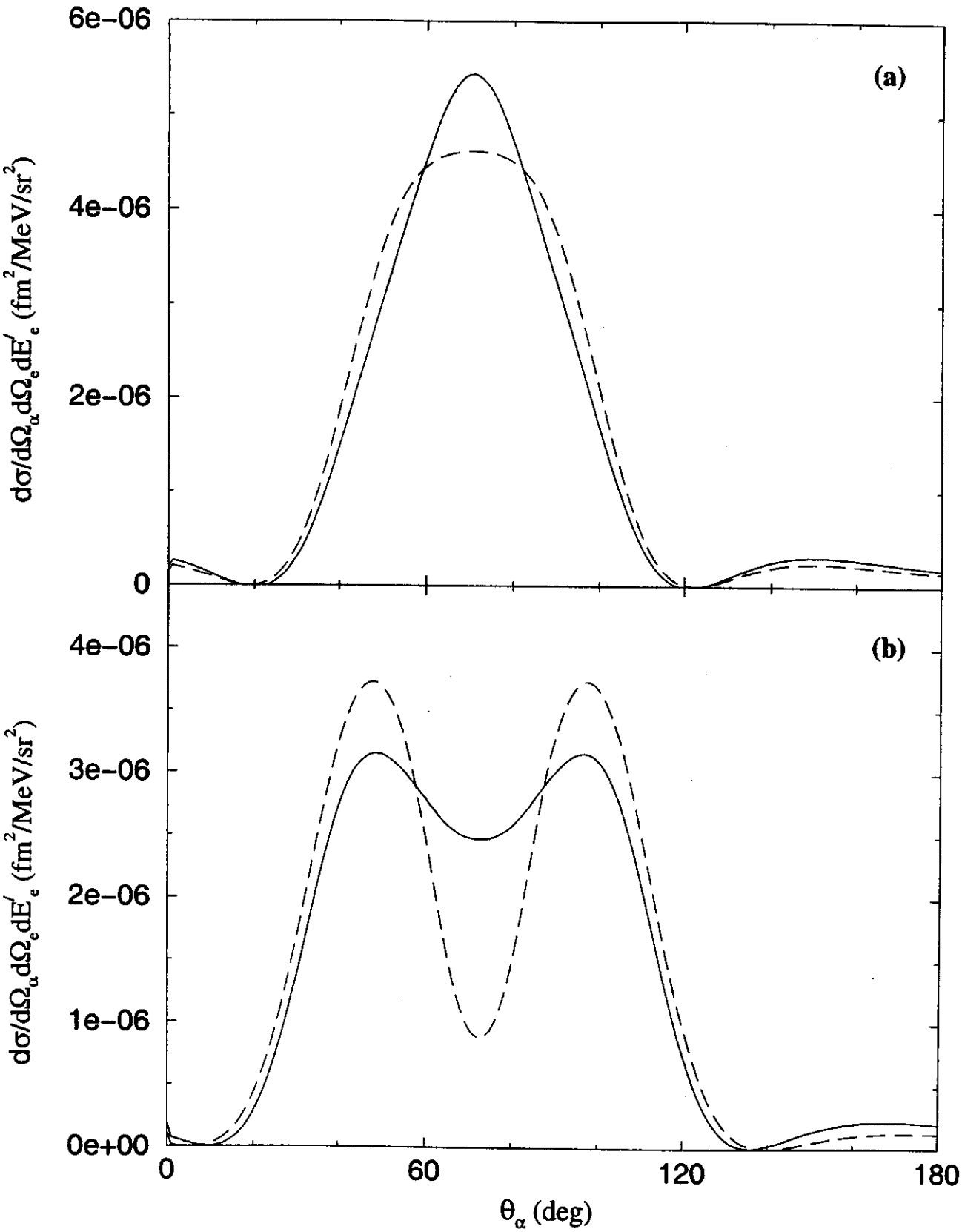
6e-06
4e-06
2e-06
0
(a)
dσ/dΩ_α dΩ_e dE'_e (fm²/MeV/sr²)
4e-06
3e-06
2e-06
1e-06
0e+00
(b)
0
60
120
180
θ_α (deg)

Fig. 9

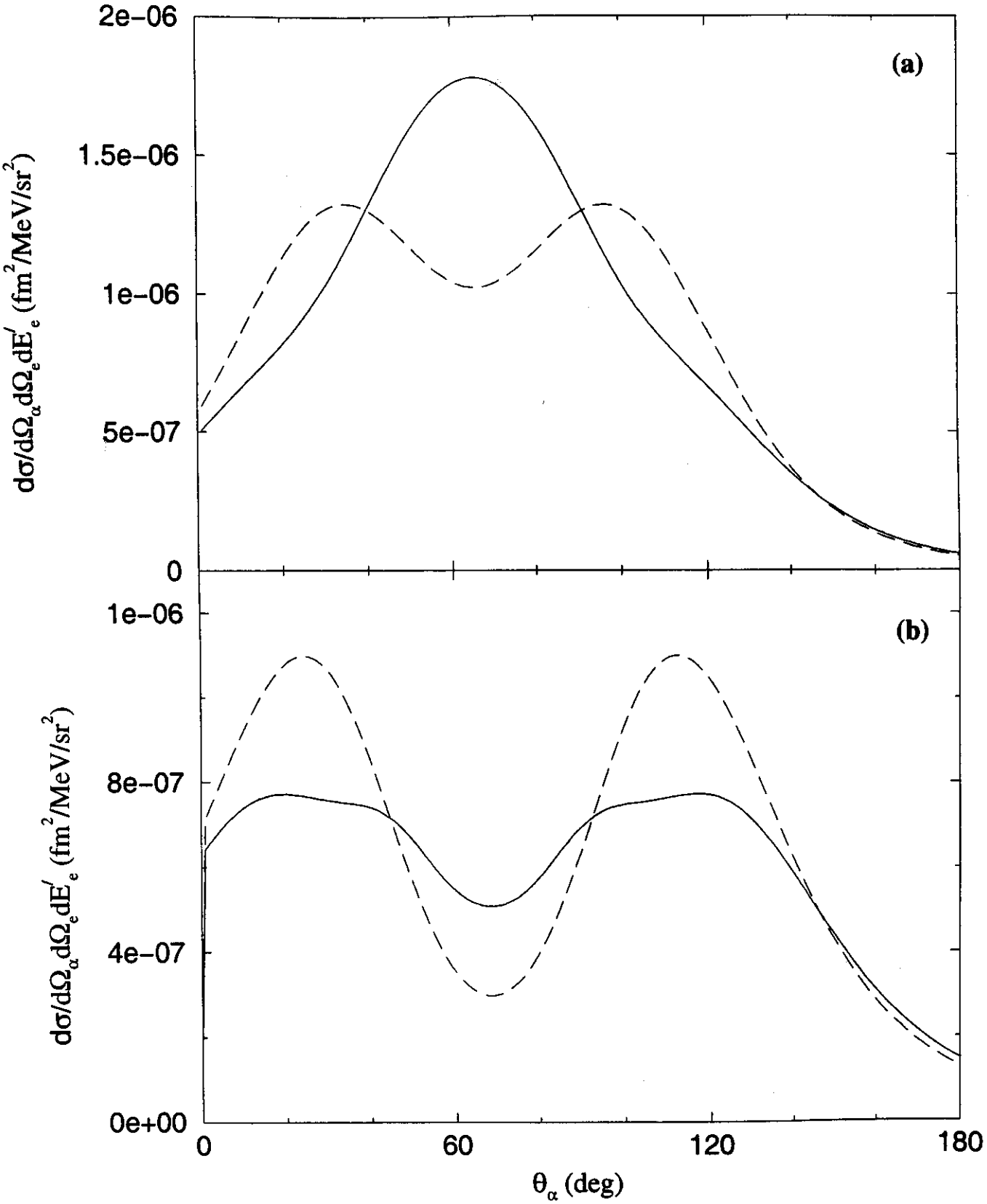
2e-06
1.5e-06
1e-06
5e-07
0
(a)
dσ/dΩ_α dΩ_e dE'_e (fm²/MeV/sr²)
1e-06
8e-07
4e-07
0e+00
(b)
dσ/dΩ_α dΩ_e dE'_e (fm²/MeV/sr²)
0
60
120
180
θ_α (deg)

Fig. 10